Deltares

Modelling of nutrient load scenarios and transboundary nutrient transport

A model study for OSPAR regions II, III and IV

Modelling of nutrient load scenarios and transboundary nutrient transport
A model study for OSPAR regions II, III and IV

Author(s)
Theo Prins
Anouk Blauw
Lauriane Vilmin
Luuk van der Heijden
Sonia Heye
Lora Buckman

Modelling of nutrient load scenarios and transboundary nutrient transport
A model study for OSPAR regions II, III and IV

Client	Rijkswaterstaat Water, Verkeer en Leefomgeving
Contact	Mw. dr. L. Enserink
Reference	31188450
Keywords	NE Atlantic, eutrophication, ecosystem model

Document control	
Version	1.1
Date	06-10-2023
Project nr.	11209731-000
Document ID	11209731-000-ZKS-0003
Pages	69
Classification	
Status	final

Author(s)

	Theo Prins	
	Anouk Blauw	
	Lauriane Vilmin	
	Luuk van der Heijden	
	Sonia Heye	
	Lora Buckman	

Summary

As part of the Quality Status Report on the state of the marine environment in the northeast (NE) Atlantic, OSPAR applied the Comprehensive Procedure for the 4th eutrophication assessment. This assessment is based on a new and coherent set of threshold values for eutrophication indicators, new assessment areas and satellite data of chlorophyll-a in addition to *in situ* monitoring data of nutrients, chlorophyll-a and oxygen. The new, coherent, set of eutrophication thresholds is based on ensemble modelling work by several OSPAR countries organized by the OSPAR Intersessional Correspondence Group on Ecological Modelling (ICG-EMO).

The next step after the QSR assessment is the selection of measures to reduce nutrient inputs to those assessment areas that are classified as eutrophication problem areas. To this end, maximum allowable inputs (MAI) for these assessment areas need to be determined, which will form the basis for decisions on measures to achieve the required reduction of nutrient loads to each assessment area.

In this report, quantitative information on the relative contribution of each specific river to the nutrient concentrations in the assessment areas is derived to assess the effectiveness of load reduction per river source. With the Deltares hydrodynamical model and coupled biogeochemical model, we calculated the relative contribution of 24 geographical groups of riverine sources and, in addition, the contribution of atmospheric deposition, the Atlantic Ocean and outflow from the Baltic Sea to the nutrient concentrations in the assessment areas. Riverine nutrient loads used in this model study were aligned with the riverine loads reported by Contracting Parties in OSPAR's RID database. The results showed that river plumes and some coastal assessment areas showed the strongest influence from nearby rivers, whereas the influence of the natural background from the Atlantic Ocean was dominant in offshore waters. Many assessment areas were influenced by long-distance nutrient transport where several larger rivers had a significant contribution to the nutrient concentrations in those areas. Atmospheric deposition of nitrogen was a significant source as well in all areas except the more remote oceanic waters. The results from this study were in line with spatial patterns observed in earlier studies on nutrient transport and are now based on riverine loads that are consistent with the loads in the OSPAR RID database. The results are a basis for further work to establish Maximum Allowable Inputs of nutrients.

For some countries there were substantial differences between the nutrient loads in the RID database and the nutrient loads that have previously been used in the ICG-EMO modelling group. Those differences have strong impacts on the model results. For the acceptance of the model results, harmonisation of river loads is urgently needed.

To increase our understanding of the dose-response relation between nutrient and chlorophyll concentrations at sea, a statistical analysis based on *in situ* data from the Dutch part of the North Sea over a 40-year period was carried out and nutrient load scenarios were applied in a model analysis. The results showed that chlorophyll concentrations decrease with lower N and P concentrations. In coastal waters, P-limitation of phytoplankton growth is more likely. Further offshore, in areas with lower freshwater influence, the probability of N-limitation increases.

Acknowledgments
This study was supported by the European Maritime and Fisheries Fund

European Union, European Maritime and Fisheries Fund

Contents

1 Introduction

1.1 Background

The European Marine Strategy Framework Directive (MSFD) aims to achieve a good environmental status (GES) of all European marine waters. For the description of GES eleven descriptors are defined. One of the descriptors in the MSFD is D5, Eutrophication: “Human-induced eutrophication is minimised, especially adverse effects thereof, such as losses in biodiversity, ecosystem degradation, harmful algae blooms and oxygen deficiency in bottom waters”. Excess nutrients introduced into the sea by human activities can disturb the balance between nutrient availability and the growth of marine plants and animals in ecosystems, resulting in eutrophication (OSPAR 2023).
The regional sea convention for the Northeast Atlantic, OSPAR, recently published the quality status report (QSR) on the state of the marine environment in the OSPAR area[1]. The QSR forms the joint basis for MSFD reporting on GES (article 8) by the Netherlands and OSPAR Contracting Parties in 2024.
As part of this QSR an assessment of the eutrophication status of the NE Atlantic was made. This assessment is based on a new and coherent set of threshold values for eutrophication indicators, new assessment areas and satellite data of chlorophyll-a in addition to *in situ* monitoring data of nutrients, oxygen and chlorophyll-a.
The new, coherent, set of eutrophication thresholds is based on ensemble modelling work by several OSPAR countries organized by OSPAR intersessional correspondence group on ecological modelling: ICG-EMO (Lenhart *et al.* 2022, OSPAR 2022, van Leeuwen *et al.* 2023). Deltares took part in this modelling work on behalf of the Netherlands with the 3D Dutch Continental Shelf Model – Flexible Mesh (3D DCSM-FM) coupled physical-biogeochemical model for the greater North Sea.

The next step after the QSR assessment is the definition of measures to reduce nutrient inputs to assessment areas that are classified as eutrophication problem areas. To this end, maximum allowable inputs (MAI) for these assessment areas need to be defined. Riverine nutrient loads and atmospheric deposition of nitrogen are the main anthropogenic sources of nutrients in the NE Atlantic. The maximum allowable loads will form the basis for decisions on measures to achieve the required reduction of nutrient loads to each assessment area.

In a recent common workshop of the OSPAR working groups ICG-EMO and ICG-EUT, in Hamburg (22 – 23 March 2023), approaches have been discussed on how the MAI’s can be derived from a new set of model simulations coordinated by ICG-EMO. This work addresses OSPAR’s Operational Objective S1.O3: *By 2024 identify and quantify relevant sources, including transboundary transport, and agree nutrient reduction needs for each Contracting Party to [not exceed/stay below] the maximum input levels, reporting on progress in 2025 and regularly thereafter*.
In the Hamburg workshop several follow-up actions were identified:

a) Analysis of ICG-EMO’s model results to further establish dose-response relations between nutrient loads and chlorophyll concentrations at sea.
b) Model simulations of various nutrient load scenarios to improve our understanding of the dose-response relations between riverine nutrient loads and nutrient and chlorophyll concentrations at sea.
c) Quantification of the maximum allowable inputs (MAI) for the assessment areas (in particular, the areas with eutrophication problems).

[1] https://oap.ospar.org/en/ospar-assessments/quality-status-reports/qsr-2023/

d) Estimate the contribution of nutrient sources (river basins, direct discharges, atmospheric deposition) to the total nutrient inputs to the assessment areas.

The final aim of the work by ICG-EMO is to establish dose-response relationships between nutrient loads and the concentrations of chlorophyll (and where possible, other indicators of eutrophication effects like dissolved oxygen). This will be the basis to identify the maximum allowable input for a specific assessment area. In combination with estimates of the relative contribution of nutrient sources (river basins), the maximum allowable input for an assessment area can be translated to maximum allowable loads for each river basin and, consequently, required load reductions for these river basins (see Figure 1-1).

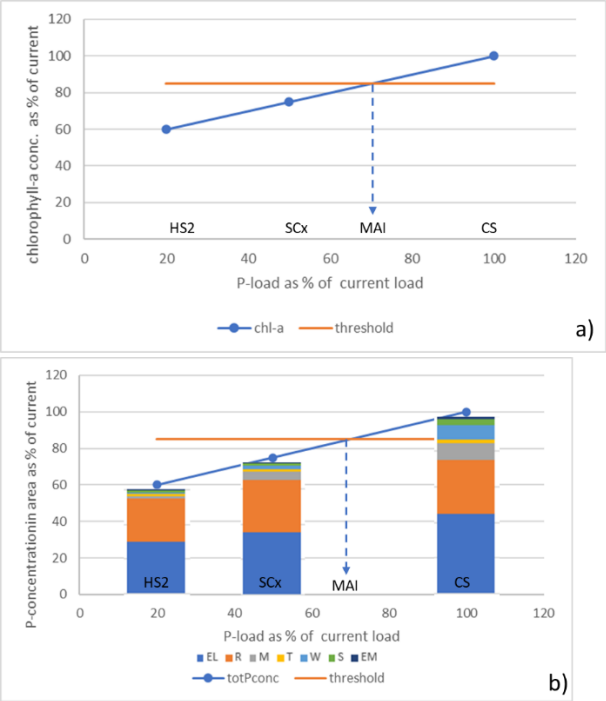

Figure 1-1 Hypothetical example showing the dose-response relation between nutrient load and chlorophyll concentration and the derivation of the maximum allowable load (MAI) in panel a) and the contribution of nutrient sources to the loads in panel b. The colours in panel b represent the contribution by different river sources, the bars represent different scenarios of nutrient loads.

With this report, Deltares contributes to the proposed follow-up actions of ICG-EMO by carrying out some exploratory model studies focused on above mentioned questions b and d. This report describes the approach and results of this modelling work by Deltares.

1.2 Objectives

Deltares has been commissioned by Rijkswaterstaat to further support the work of ICG-EMO by application of the 3D DCSM-FM model in nutrient load scenarios and by contributing to ICG-EMO reporting to OSPAR.

The objective of this study is to contribute to the estimation of MAIs by OSPAR ICG-EMO based on model results from the 3D DCSM model, by the following activities:

- Quantify transboundary nutrient transport.
  - This is done by tracer simulations of nutrient loads (total N and total P) to determine the contribution of each source (river basins, etc.) to each of the OSPAR COMP4

assessment areas. In the follow-up work on maximum allowable loads by ICG-EMO, the results of these simulations help to identify the nutrient sources contributing to excess nutrient loads in the assessment areas with eutrophication problems.

- Determine the effect of nutrient reductions on eutrophication indicators.
  - Simulations with an updated version of the physical-biogeochemical 3D DCSM-FM model are carried out to estimate the chlorophyll response to nutrient load reduction. The reduction scenario represents river nutrient loads 50% higher than the loads under the pre-eutrophic conditions in scenario HS2 in the previous ensemble modelling under ICG-EMO as reported by Lenhart et al. (2022).
- Analysis of the response of chlorophyll to nutrient load reductions.
  - Observation data and model results are analysed to establish the response of chlorophyll to changes in nutrient loads in various OSPAR areas.

1.3 Outline of the report

Chapter 2 gives a description of the aggregation of nutrient sources for the tracer study, the definition of nutrient loads, model improvements made after the previous application under ICG-EMO (Lenhart *et al.* 2022) and the *in situ* data used for analysis.
The results of the nutrient tracer study are described in Chapter 3 and give estimates of various sources to the nutrient concentrations in the assessment areas.
The results of the model simulations for the current state (years 2015-2017) are compared to observations, for validation, in Chapter 4.
In Chapter 5, the results of the nutrient load reduction scenario are compared to the current state run to establish the effects of nutrient load reductions on the eutrophication status of the NE Atlantic.
An analysis of the response of chlorophyll concentrations to the changes in nutrient loads over the last decades in the Dutch part of the North Sea is presented in Chapter 6.
Chapter 7 discusses the results of this study. Recommendations for the follow-up are given in Chapter 8.

2 Methods

2.1 Aggregation of nutrient sources

In the ICG-EMO modelling exercise (Lenhart *et al.* 2022, van Leeuwen *et al.* 2023), data from the ICG-EMO database on riverine nutrient loads of 368 rivers have been used. For the nutrient tracer modelling, it was necessary to reduce this number of individual sources to limit the computational effort to a feasible level. Therefore, the individual river sources were aggregated into groups of rivers based on country, assessment area(s) they flow into and size of individual river loads. If two or more of the largest rivers from the same country flow into the same assessment area, several tracers were defined. This was the case for the Thames and Humber in the UK and the Weser, Ems and Elbe in Germany. Two tracers were defined for the Netherlands: one representing the loads entering directly into the southern North Sea and one representing the loads to the Wadden Sea.
After consultation of the ICG-EMO convenor, a spatial aggregation of sources was made as shown in Figure 2-1.
In addition to the river sources, tracers were added in the model runs to identify:
1) the inflow from the Atlantic Ocean,
2) the inflow from the Baltic Sea and
3) atmospheric deposition (only for nitrogen).

Table 2.1 gives a more detailed description of the aggregated groups of rivers.

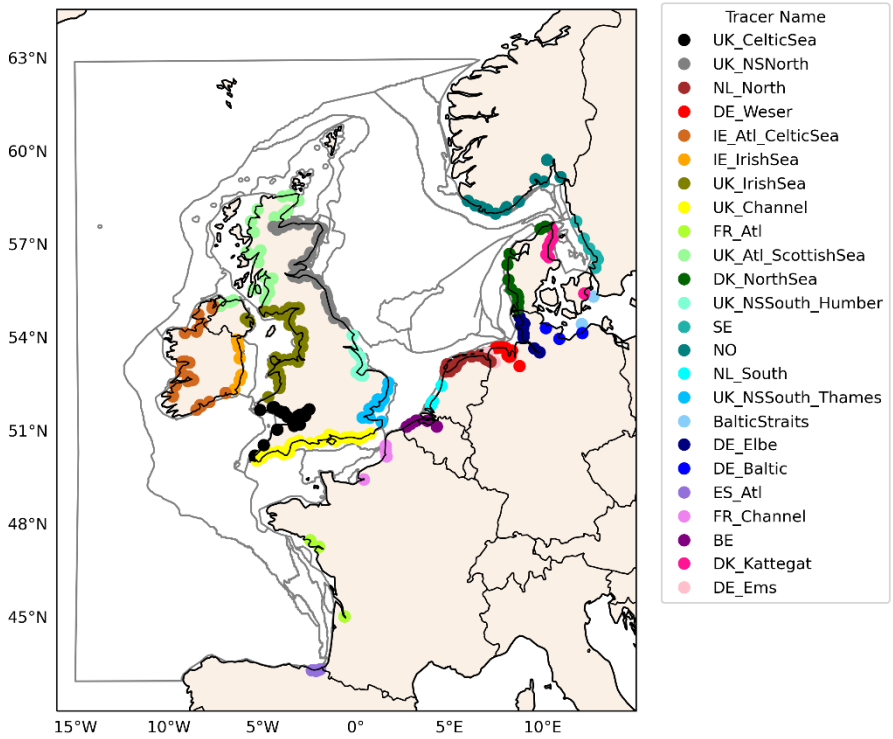

Figure 2-1 Map showing the aggregation of the individual river sources in the ICG-EMO database into 24 groups. The grey lines show the borders of the assessment areas.

Table 2.1 Tracer names of the aggregated groups of river sources and description of the rivers included in the groups.

Tracer name	Country	Description
Atlantic boundary inflow	-	Atlantic boundary inflow
BalticStraits	-	Baltic boundary inflow at Dars and Drogden sills
NO3	-	Atmospheric nitrogen deposition
NO	Norway	All Norwegian rivers in model domain
SE	Sweden	All Swedish rivers in model domain
DK_Kattegat	Denmark	All Danish rivers discharging to Kattegat
DK_NorthSea	Denmark	All other Danish rivers
DE_Baltic	Germany	All German rivers discharging to Baltic Sea
DE_Elbe	Germany	Elbe and nearby German rivers
DE_Weser	Germany	Weser and nearby German rivers
DE_Ems	Germany	Ems and nearby German rivers
NL_North	Netherlands	Lake IJssel and nearby Dutch discharges
NL_South	Netherlands	Rhine and Meuse outlets near Rotterdam
BE	Belgium	All Belgian rivers, including the Scheldt
Fr_Channel	France	French rivers to Channel north of Brest
Fr_Atlantic	France	French rivers to Atlantic south of Brest
Es_Atlantic	Spain	Rivers on Spanish North coast
IE_Atl_CelticSea	Ireland	Irish rivers to the Atlantic Ocean and Celtic Sea
IE_IrishSea	Ireland	Irish rivers to Irish Sea
UK_IrishSea	United Kingdom	UK rivers to the Irish Sea
UK_Atl_ScottishSea	United Kingdom	UK rivers to the Atlantic Ocean and Scottish Sea
UK_NSNorth	United Kingdom	UK rivers to northern North Sea
UK_NSSouth_Humber	United Kingdom	UK rivers to southern North Sea, near Humber
UK_NSSouth_Thames	United Kingdom	UK rivers to southern North Sea, near Thames
UK_Channel	United Kingdom	UK rivers to Channel
UK_Celtic	United Kingdom	UK rivers to Celtic Sea

2.2 Adjustments of river loads to RID data

In the previous ICG-EMO modelling exercise, river loads were derived from the ICG-EMO river load database that is maintained by Sonja van Leeuwen at NIOZ (Lenhart *et al.* 2022, van Leeuwen *et al.* 2023). This database has a higher level of detail than the OSPAR RID database[2] (see e.g. Axe *et al.* 2023): the ICGEMO database contains a higher number of individual rivers and has a higher temporal resolution than the annual data in the RID database.

However, as the ICG-EMO work will have to provide the basis for decisions on nutrient reduction measures, it was decided that the follow up of the ICG-EMO modelling work should be based on total river loads that are better aligned with the data in the RID database (HASEC 2023).

[2] RID - Nutrient Inputs From Land-Based (Diffuse and Point) Sources https://oap.ospar.org/en/ospar-monitoring-programmes/cemp/cemp-appendices/theme-e-eutrophication/inputs-nutrients/rid-nutrient-inputs/

As the alignment of the ICG-EMO database with the RID data was not finished yet, we used an intermediate solution as discussed with the ICG-EMO convenor and with Rijkswaterstaat. It was agreed in ICG-EMO that model runs would focus on the years 2012-2017, with 2012-2014 as spin-up years. Years after 2017 were not included in the assignment because for those years the ICG-EMO river load data are not fully available yet.
Data from the RID database for the years 2012-2017 were downloaded. These data and the ICG-EMO-derived model river loads (calculated as done in Lenhart et al., 2022) were aggregated at the same spatial scale, based on RID assessment areas (Figure 2-2). This provides an annual total-N and total-P load for each area and for each data source. Average yearly loads for the period 2015-2017 per RID assessment area and per data source are plotted in Figure 2-3.

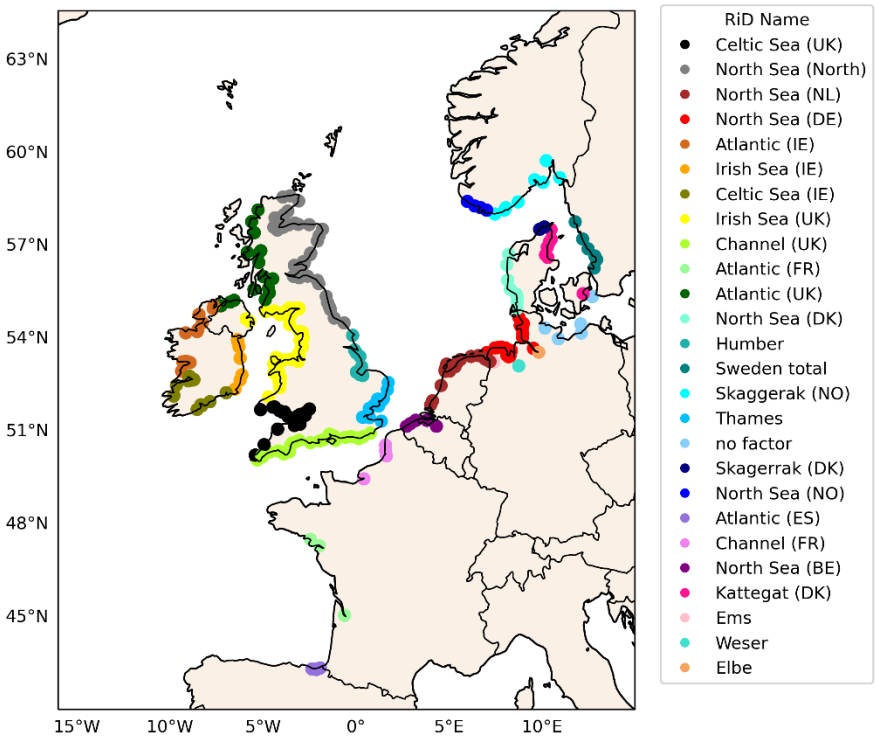

Figure 2-2: Map showing the aggregation of the individual river sources in the ICG-EMO database over the different RID assessment areas.

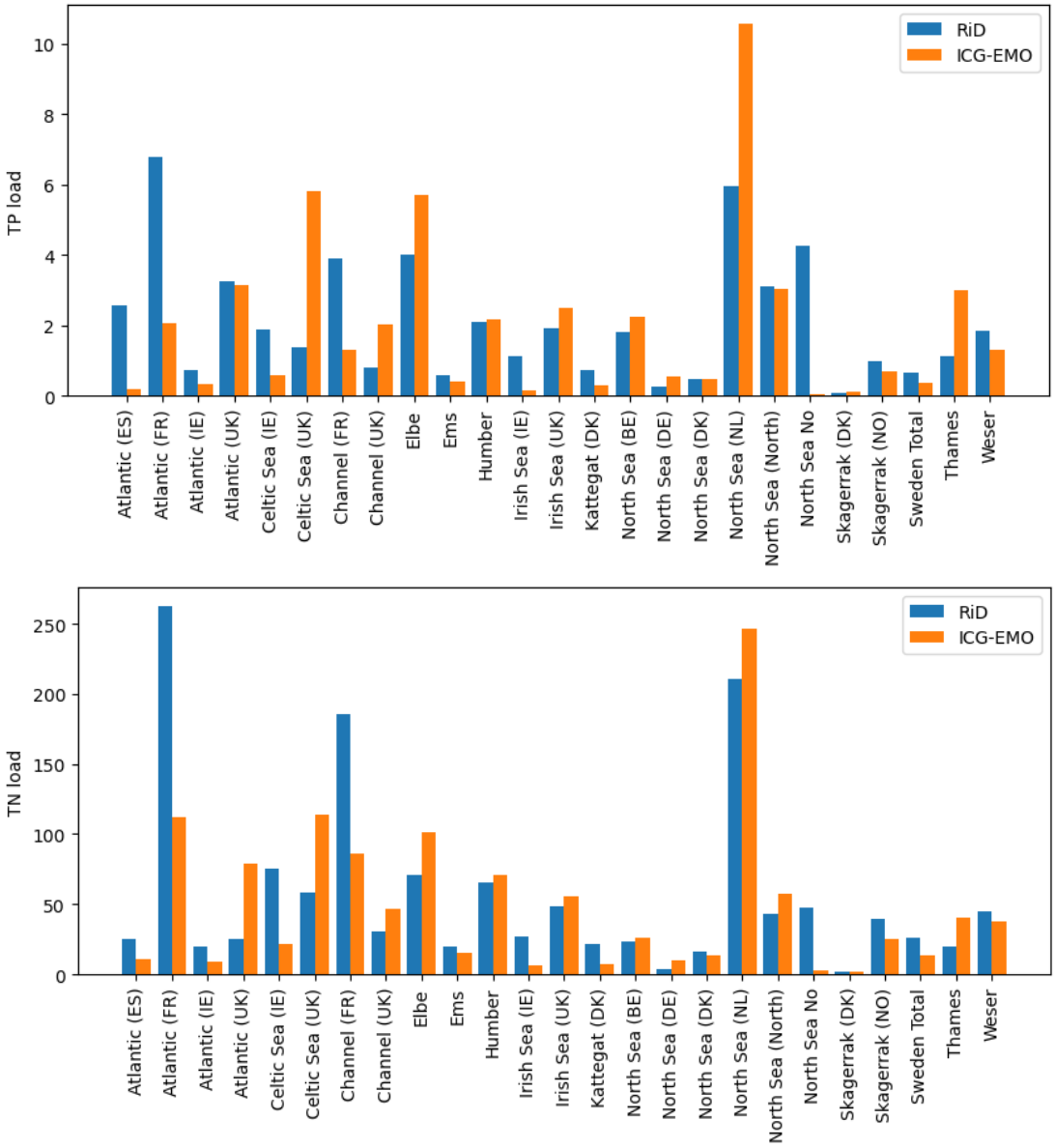

Figure 2-3: Average yearly total P and total N loads (in kton/year) for the period 2015-2017 per RID assessment area and per data source (RID data and ICG-EMO-derived loads)

From the comparison of the RID data with the ICG-EMO data (Figure 2-3), a year-by-year scaling factor was derived for each aggregated group of rivers. With this scaling factor, the ICG-EMO river loads were adjusted so that the total load in each aggregated river group matched the total loads in the RID database. In countries where the ICG-EMO database is very detailed (with more river inputs than reported in the RID database), such as in the UK and in the Netherlands, this led to a downwards correction. In countries for which the ICG-EMO database is less complete, such as Spain, France and Norway, reported RID loads are substantially higher than ICG-EMO loads. In those areas, correction factors applied to the model inputs led to an increase in nutrient loads with respect to the previous simulations reported in Lenhart et al. (2022). Annex B gives an overview of the yearly loads from each source and the correction factors applied to the model nitrogen and phosphorus inputs to be consistent with RID reported loads.

For each N-component (NO_3, NH_4, PON, DON, POC and DOC) the same scaling factor derived for total-N was applied. For each P-component (PO_4, POP, DOP) the same total-P scaling factor was used.
Dissolved organic nitrogen (DON), phosphorus (DOP) and carbon (DOC) variables were included in the updated version of the model (see §2.5 for more details), while they were not accounted for in Lenhart *et al.* (2022). However, this addition did not impact TN and TP river loads in the model: a fraction of the total organic pool, initially all attributed to the particulate variables, was now attributed to the dissolved organic variables.

2.3 Model boundaries and initial conditions

Model boundaries for nitrogen and phosphate concentrations were based on CMEMS model output, both in the tracer simulations and in the simulations with the full ecological model. Total-N and total-P concentrations at the offshore boundaries were forced using the monthly CMEMS Global Ocean Biogeochemistry Hindcast product. Total-N concentrations were calculated as the sum of NO_3^-, PON and DON. Total-P concentrations were calculated as the sum of PO_4^{3-}, POP and DOP. While NO_3^- and PO_4^{3-} are directly available from the CMEMS product, PON, POP, DON and DOP were derived from the CMEMS phytoplankton carbon content variable, as described by Zijl *et al.* (2021), Zijl *et al.* (2023b) and in §2.6. These concentrations were included as a tracer for 'offshore waters' in the tracer model.
Initial total-N and total-P over the model domain were defined based on CMEMS data available for January 2012. To improve model accuracy in the first simulation years, CMEMS data for NO_3^- and PO_4^{3-} were overwritten, for the central North Sea, by spatially interpolated winter average concentrations extracted from EMODnet, similar to what was done in the runs in Lenhart *et al*. (2022). Initial total-N and total-P concentrations were represented by an "initial" tracer that allowed to have an idea of how long it took for different parts of the domain to be flushed (residence times). The model was spun up for 3 years, from 1 January 2012 to 1 January 2015. Model runs were then carried out for 1 January 2015 to 1 January 2018 for the analysis of the model results.

2.4 Nutrient tracer study

In the nutrient tracer modelling, nitrogen and phosphorus were labelled based on the river group as source (Table 2.1). This method of labelling of nutrients has been applied in previous modelling work to identify the origin of nutrients at specific locations in the marine environment (Blauw *et al.* 2006, Lacroix *et al.* 2007, Lenhart *et al.* 2010, Painting *et al.* 2013, Los *et al.* 2014, Dulière *et al.* 2017, Lenhart & Große 2018, Ménesguen *et al.* 2018).
In this study, we quantified the relative contribution of river sources at the spatial scale of the new OSPAR assessment areas that are used in OSPAR's eutrophication assessment (OSPAR 2022). Annex A shows maps of the assessment areas.
Aditionally, we present results for areas in the Wadden Sea, where also information is needed by Rijkswaterstaat on the origin of nutrients.
The relative contribution was calculated from the average concentrations over 2015-2017, after a 3-year spin-up. During the spin-up, initial concentrations (see §2.3) were gradually replaced by inputs from riverine and atmospheric sources and from the Atlantic Ocean and Baltic Sea.
In the tracer model, only conservative transport (i.e., excluding biogeochemical/ecological processes) was applied to limit the computational effort of the model simulations. Earlier model applications showed that estimates of the relative contribution of sources based on conservative transport have only minor deviations from the results based on an ecological model including those processes (Blauw *et al.* 2006).

For the total-N tracer runs, in addition to offshore, initial and all river-bound tracers, a tracer for atmospheric deposition was included. The latter was forced as a 2D field, resulting from

the addition of wet and dry deposition of reduced and oxidized N forms from EMEP for the year 2017. Those data on atmospheric deposition were also used in Lenhart et al. 2022).

2.5 Nutrient load scenarios

In the ensemble model exercise of ICG-EMO (Lenhart *et al.* 2022), current state was calculated for the years 2009-2014. As historic nutrient load scenario, two scenarios (HS1 and HS2) were applied that represented pre-eutrophic conditions at the end of the 19th century. The two 'pre-eutrophic' scenarios differed in total-P loads for the Netherlands, Germany and Denmark (Lenhart *et al.* 2022, van Leeuwen *et al.* 2023). Based on the results of the pre-eutrophic scenario, thresholds for dissolved inorganic nitrogen and phosphorus and for chlorophyll were derived for each of the assessment areas by adding 50% to the pre-eutrophic concentrations (Lenhart *et al.* 2022, OSPAR 2022, van Leeuwen *et al.* 2023).

Here, we carried out a current state simulation for the more recent years 2015-2017 (with 2012-2014 as spin-up years). We compared this current state with a scenario with reduced nutrient loads. The reduced nutrient load scenario was run with nutrient loads 50% higher than the nutrient loads in the pre-eutrophic scenario HS2 used by Lenhart *et al.* (2022). In this report we refer to this reduced nutrient scenario as 'HS2+50%'. The rationale for choosing this scenario was that it comes close to the derived assessment thresholds (pre-eutrophic concentration + 50%). The choice for scenario HS2 instead of scenario HS1 was made to explore the effect of a larger difference with current loads.
In the HS2+50% scenario only the nutrient loads from rivers and the Baltic straits were changed compared to the current state simulation. Nitrogen atmospheric deposition and nutrient inputs from the Atlantic offshore boundary were not changed.

Figure 2-4 shows the total-P and total-N loads per country in the HS2+50% scenario, expressed as percentage of the current (2012-2017) loads. As in many cases total-P loads have already decreased substantially since the early 1990s, the HS2+50% scenario loads of total-P are closer to current loads than the total-N loads. In addition, the difference between total-P loads in Scenario HS2 and in the current state varied considerably between countries. For example, for France the TP loads in the HS2 scenario ranged from 71% (Seine) to 92% (Loire) of current loads (Lenhart *et al.* 2022). Consequently, in some cases adding 50% to the loads of the HS2 scenario resulted in loads in the HS2+50% scenario that are higher than current loads. In the previous model exercise by ICG-EMO (Lenhart *et al.* 2022), rivers with pre-eutrophic loads higher than current loads (mainly Scottish areas with declines in population) were kept at the same level as current loads. In this study we allowed loads in the HS2+50% scenario to be higher than current loads as we wanted to explore nutrient-chlorophyll relations in this specific scenario.
Because of the differences between rivers in loads under pre-eutrophic and current conditions, the loads in the HS2+50% scenario, expressed as percentage of current loads, differed substantially between rivers. An example for the five largest rivers is shown in Table 2.2. This example also shows that for French rivers the HS2+50% scenario resulted in TP loads higher than current loads.

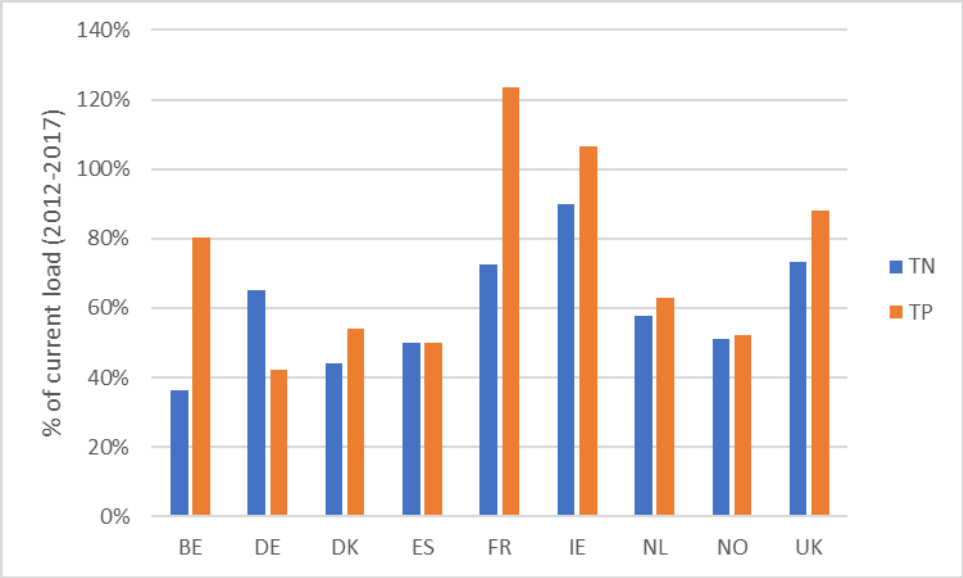

Figure 2-4: Loads of total-P and total-N I the HS2+50% scenario in percent of current loads.

Table 2.2 Average TN and TP loads in the current state (2012-2017), in the HS2+50% scenario, and HS2+50% loads as percentage of current loads. Loads for Rhine and Meuse are combined as Nieuwe Waterweg and Haringvliet discharge a mixture of both rivers.

		Average load 2012-2017		Average load HS2+50%			
		kton/year		kton/year		% of current	
Country	River	TN	TP	TN	TP	TN	TP
FR	Loire	287	6,1	216	8,4	75%	138%
FR	Seine	190	3,9	128	4,1	67%	107%
NL	Rhine/Meuse	166	4,2	103	2,4	62%	57%
DE	Elbe	90	4,5	69	1,8	77%	39%
UK	Humber	41	2,2	21	1,1	51%	50%

2.6 Model upgrade

The model configuration/schematization applied in this study is similar to the model schematization used in the previous ICG-EMO work (van Leeuwen *et al.* 2023), with some adjustments as described below. The model domain and spatial resolution of the model grid is shown in Figure 2-5. The hydrodynamical model D-FLOW FM calculates the transport processes of water and substances. The water quality processes are calculated by the coupled biogeochemical model GEM (Generic Ecological Model). GEM has been developed on the basis of the generic software system Delft3D-WAQ and describes light climate, nutrients, oxygen, primary production, chlorophyl and phytoplankton composition. The model has been applied in many studies on nutrients and phytoplankton in the North Sea and the Wadden Sea, including the recent ensemble modelling for ICG-EMO (Blauw *et al.* 2008, Troost *et al.* 2013, Los *et al.* 2014, Troost *et al.* 2014, van der Kaaij *et al.* 2017, van Leeuwen *et al.* 2023).

Through a statistical analysis and using target diagrams, Zijl *et al.* (2023a) showed that the addition of DOC, DON and DOP to the model (sigma-layer version used in the WOZEP project) results in a slowing down of the recycling of organic matter in the system, leading to lower availability of nutrients in the system. As a consequence, the initial overestimation of DIN concentrations at Dutch MWTL monitoring stations was slightly reduced, but most of all,

the representation of chlorophyll-a concentrations was visibly improved. In these WOZEP runs, POC concentrations (notably composed of living and dead phytoplankton biomass), which were overestimated by a factor ~4 at stations Rottumerplaat 70 km and Terschelling 10km (only stations where measurements were available), were well represented by the model, after this introduction of dissolved organic matter in the model. Based on these results from the WOZEP project, we have also implemented DOM in the upgraded model version used in this study.

In summary, the following changes to the model set-up were made in this study, compared to the previous model runs used in Lenhart *et al.* (2022):

- We rescaled the river loads from the previous model runs so that the total loads are consistent with the river loads in the OSPAR RID database. More details are given in §2.2.
- We used the latest version of the hydrodynamic 3D DCSM FM model. This implies updated bathymetry inputs and some adjustments of hydrodynamic parameter settings. Underlying hydrodynamics are consistent with the latest Deltares/Rijkswaterstaat release (Zijl *et al.* 2023b).
- DOC, DON and DOP concentrations in rivers were forced using the ratios of nutrient export estimates for European rivers from Seitzinger *et al.* (2005). We used the following ratios: DOC:POC=8:7, DON:PON=0.7:1.1, DOP:POP=0.04:0.33, DOP:DIP=0.04:0.20.
- We initialized the amount of inorganic matter in the top sediment layer (IM1S1) from model results of the sediment model used for the WOZEP research programme (Zijl *et al.* 2023a). This is more realistic than the uniform distribution that was used in earlier simulations. The amount of inorganic matter in the top sediment layer affects the burial of organic matter in the sediment.
- Turbidity related to suspended inorganic matter in the Wadden Sea was based on yearly average data from Sentinel-2 satellite (100 x 100 m) instead of MERIS. The same sinusoidal function as applied to the MERIS data over the rest of the domain (Lenhart et al. 2022), was used to derive weekly 2D fields of suspended particulate inorganic matter.

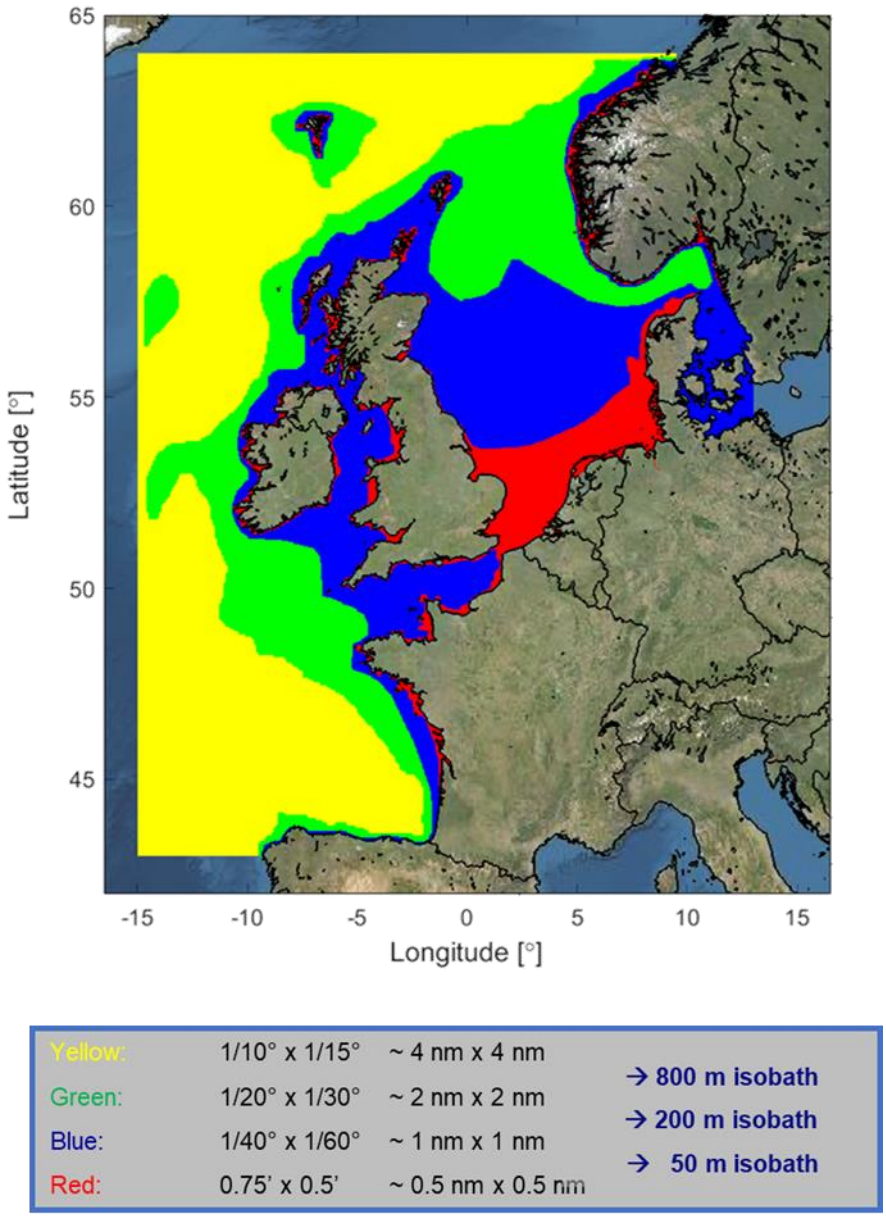

Figure 2-5 Model domain of the DFLOW-FM model for the Greater North Sea. The colours show the spatial resolution of the model grid.

2.7 Analysis of nutrient-chlorophyll relations

During the ensemble modelling work by ICG-EMO (Lenhart *et al.* 2022) the response of chlorophyll-a concentrations to nutrient reduction scenarios appeared to differ strongly between the models in the ensemble (van Leeuwen *et al.* 2023). This is illustrated in Figure 2-6, showing the relative decrease in chlorophyll-a concentrations to relative decreases in DIN and DIP concentrations in various assessment areas and in different models. In the Deltares model (red dots) and RBINS model (light blue dots) chlorophyll-a concentrations appear to respond approximately linearly to reductions in nutrient concentrations. Some other models (for example the JRC model and Oldenburg model) show much less strong responses of chlorophyll-a concentrations to nutrient reduction.

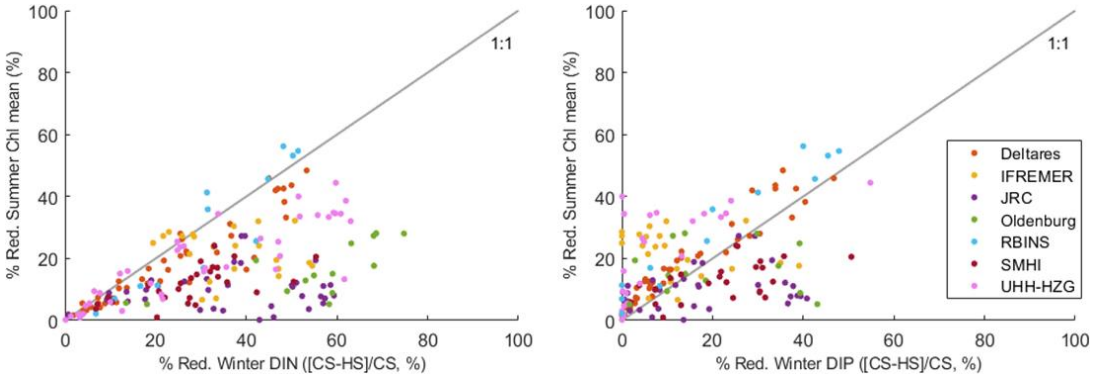

Figure 2-6: Relative reduction of growing season mean Chorophylll as a function of the relative reduction of winter DIN (A) and winter DIP (B). Each dot indicates a marine assessment area and models are represented by different colours (figure 12 from paper by van van Leeuwen et al. *2023)*

These large differences between model responses led to large uncertainties in the expected effectiveness of nutrient reduction measures and in the thresholds estimated by the ensemble of models, which is undesirable as the model results provide the scientific basis for policy implementation. Therefore, in this study we aimed to reduce the uncertainty on the chlorophyll-a response to nutrient reduction by investigating the chlorophyll-a response to historic reductions in nutrient concentrations in field observations.
To this end we used the MWTL monitoring data of Rijkswaterstaat in the Dutch part of the North Sea. These observations cover a wide range of environmental conditions and, in most cases, have consistent biweekly to monthly observations available from 1976 onwards. We have analysed the data of 12 MWTL locations with relatively good data availability for the years 1976 to 2021. These locations are listed in Table 2.3.

Table 2.3 Overview of locations used in the data analysis in this study.

MWTL location name	MWTL location code
Noordwijk 2 km from the coast	NOORDWK2
Noordwijk 10 km from the coast	NOORDWK10
Noordwijk 20 km from the coast	NOORDWK20
Noordwijk 70 km from the coast	NOORDWK70
Walcheren 2 km from the coast	WALCRN2
Walcheren 20 km from the coast	WALCRN20
Walcheren 70 km from the coast	WALCRN70
Terschelling 10 km from the coast	TERSLG10
Terschelling 100 km from the coast	TERSLG100
Terschelling 135 km from the coast	TERSLG135
Terschelling 175 km from the coast	TERSLG175
Terschelling 235 km from the coast	TERSLG235

First, we plotted all data as time series and calculated a trend using linear regression of concentrations against time. This showed very significant trends for nutrient concentrations but hardly any significant trend for chlorophyll-a concentrations. Chlorophyll-a concentrations are known to fluctuate strongly in time, particularly during spring. Therefore, biweekly to monthly observations are often not representative of the variability in chlorophyll-a concentrations. To reduce the effect of noisy data due to temporal undersampling we aggregated all data over longer periods of approximately one decade and tested for differences in means between periods with a 2-sided t-test. The time series of DIP showed many outliers at different locations. These strongly affected the calculated winter mean DIP concentrations. In order to reduce the influence of these outliers and get a more representative estimation of DIP concentrations in winter, we used the winter median values of DIN and DIP over a multi-year period. Table 2.4 shows the classification in the different periods.

Table 2.4 Overview of classification of years in 4 periods of approximately 10 years.

Period	Years included	Comment
80s	1976 - 1990	Several locations lack data for 1983-1987
90s	1991 - 2000	DIP concentrations strongly decrease between 1991 and 1993
00s	2001 - 2010	
10s	2011 - 2021	

3 Results of tracer simulations

In this chapter, we present the results of the nutrient tracer study with spatial maps showing the total nutrient concentrations and the relative contribution of the various sources to the total concentration in each assessment area.

3.1 Total phosphorus

The tracer modelling of total-P illustrated how the various river plumes affected different parts of the NE Atlantic. The influence from riverine sources was strongest along the coast near major river outflows and in the Baltic area. For all sources from Table 2.1, the contribution to the annual mean concentrations of TP was calculated at the scale of the model grid cells. A selection of the maps, focusing on the Greater North Sea, is shown in Figure 3-1.

Pie charts show the relative contribution of all sources to the average concentration of TP in each OSPAR assessment area (Figure 3-2). To improve the visibility of the contribution by specific river sources, the contribution of each river is also plotted as the percentage of the total river contribution, excluding the contribution from the Atlantic Ocean (Figure 3-3).
As was already clear from Figure 3-1, the influence of the Atlantic Ocean dominated offshore areas in the Celtic Seas, the northern part of the North Sea and OSPAR region IV Bay of Biscay and Iberian coast. Along the SE English coast and the continental coast of the North Sea the contribution of the river sources differed between assessment areas, with a gradual change following the transport pattern of the residual current.
Table 3.1 gives an overview of the relative contribution of each source to the annual mean TP concentration in each assessment area.
Figure 3.1, 3.2 and Table 3.1 show that the river plumes were generally dominated by the contribution from one or several nearby river sources. Some coastal assessment areas had a relatively large contribution from river sources (>10%), generally a mixture from several rivers. TP concentrations in the assessment areas categorised in OSPAR (2023) as shelf areas were mainly dominated by the Atlantic Ocean as source, with the exception of the assessment area CFR in the Channel. The inflow from the Baltic Sea was a substantial source in the Kattegat assessment areas.
Figure 3.2 and Table 3.1 show the importance of transboundary nutrient transport and the contribution of large remote rivers in many assessment areas, particularly in the North Sea.

The WFD water bodies in the Wadden Sea showed a large contribution from Rhine/Meuse and Lake IJssel in the Dutch part of the Wadden Sea. The river Elbe was the dominating source in the eastern part of the German Wadden Sea (Figure 3-4, Table 3.2).

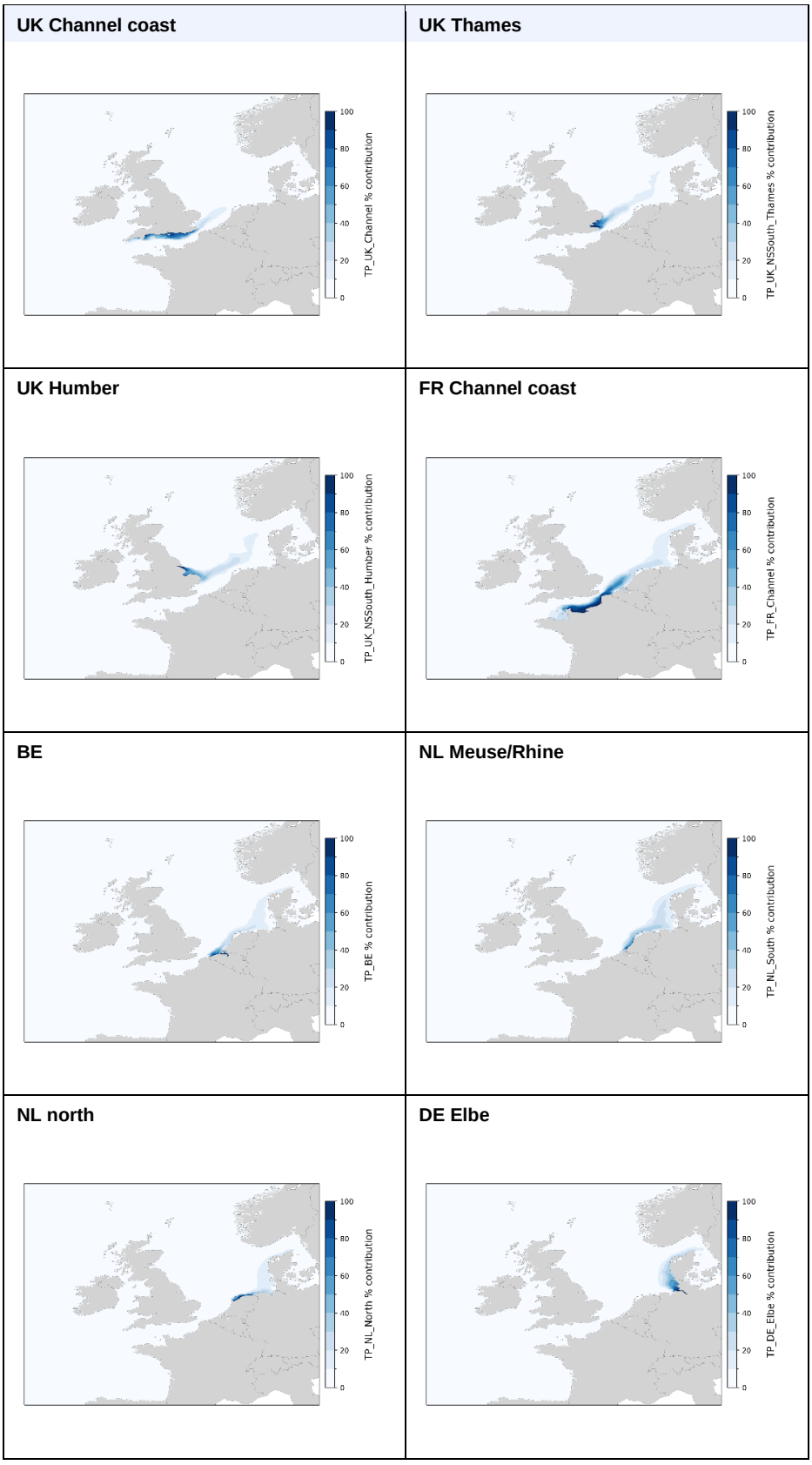

Figure 3-1 Maps showing the relative contribution (in %) of a selection of river sources to the annual mean total-P concentration.

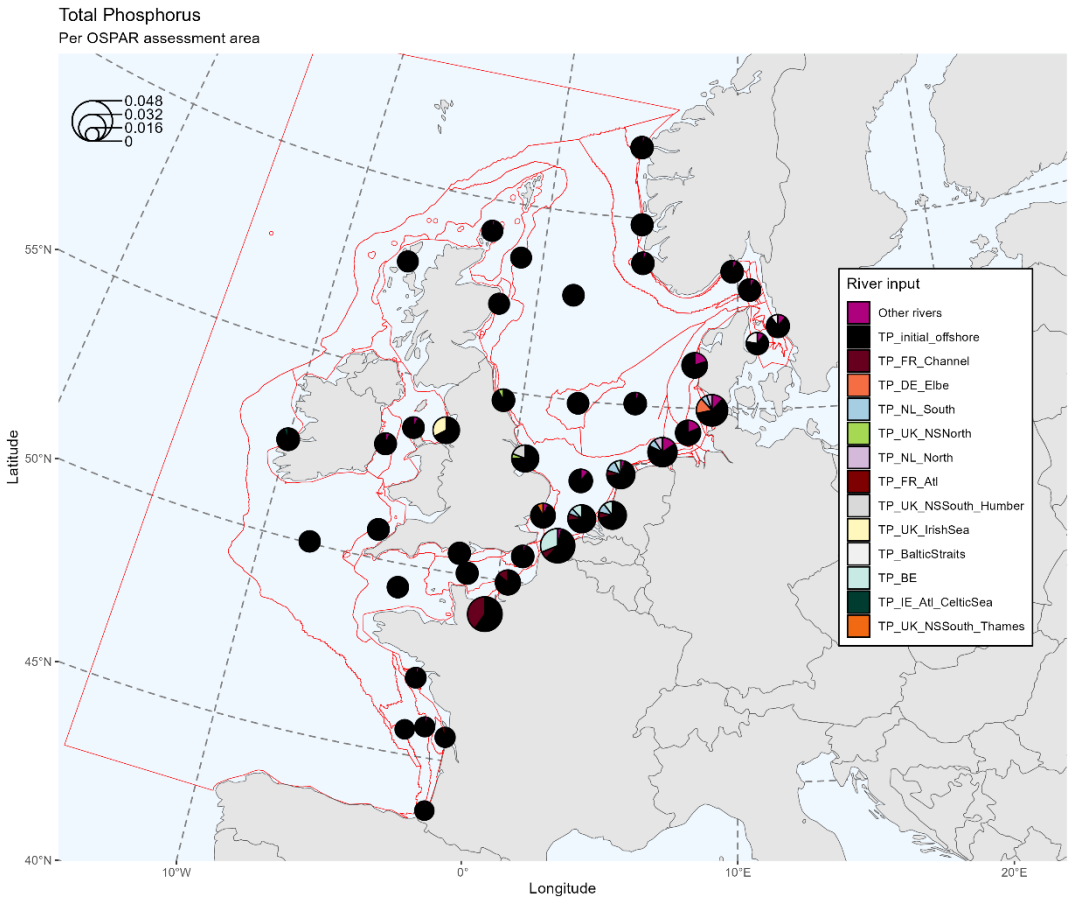

Figure 3-2 Relative contribution of the sources (see Table 2.1) to the annual mean total-P concentration in each COMP4 assessment area. The size of the pie chart indicates the concentration in an assessment area, the pies reflect the contribution of each source. "Other rivers" is the sum of rivers with a contribution to total-P concentration <5%.

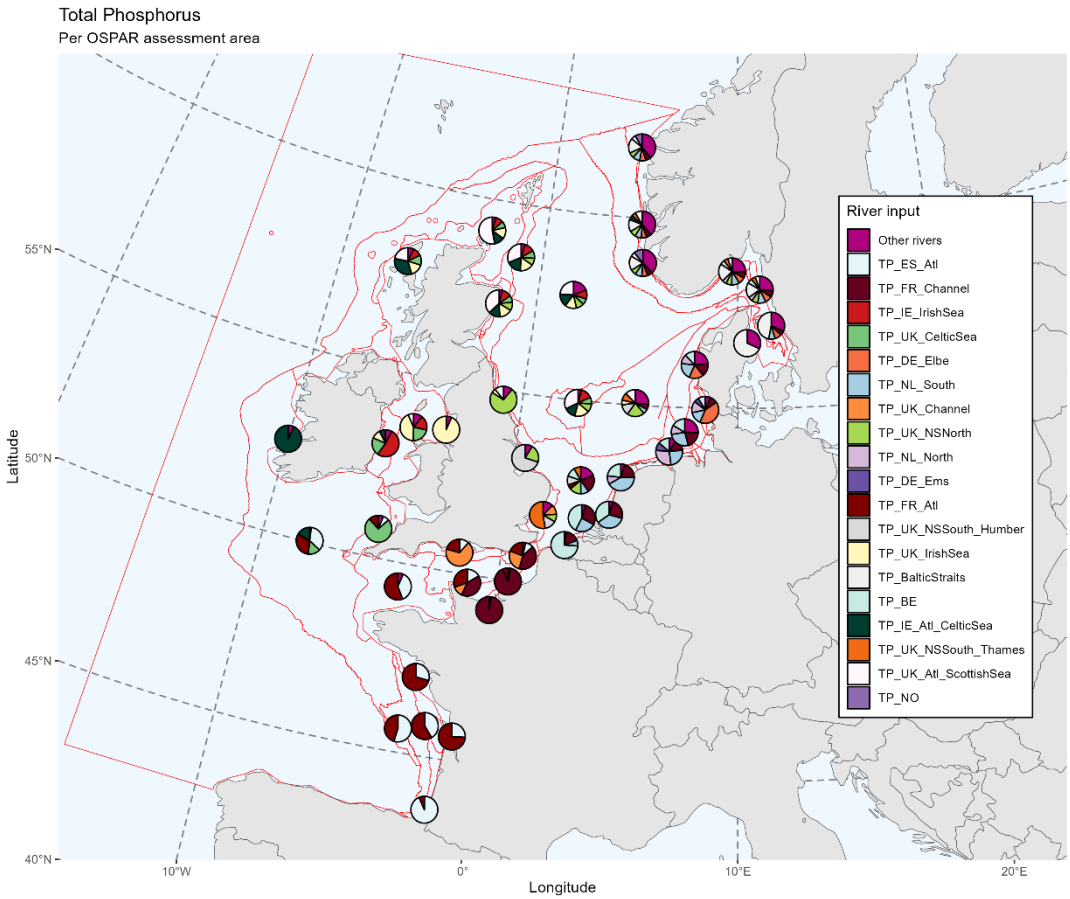

Figure 3-3 Relative contribution of the river sources (see Table 2.1) to the annual mean total-P concentration in each COMP4 assessment area. The pies reflect the contribution of each river source, with the contribution from the Atlantic Ocean excluded. "Other rivers" is the sum of rivers with a contribution to total-P concentration <5%.

Table 3.1 Overview of the relative contribution of sources to the TP concentration in each OSPAR assessment area. Contributions from rivers >1% are highlighted in grey. The contribution from the Atlantic Ocean is highlighted in orange when it is <90%.Assessment areas are categorised according to OSPAR (2023).

Category	COMP4 assessment area	Area ID	ES_Atl	FR_Atl	FR_Channel	UK_Channel	BE	NL_South	NL_North	DE_Ems	DE_Weser	DE_Elbe	DK_NorthSea	DK_Kattegat	SE	NO	UK_Thames	UK_Humber	UK_NorthSeaNorth	UK_Atl_ScottishSea	UK_CelticSea	UK_IrishSea	IE_IrishSea	IE_Atl_CelticSea	Atlantic Ocean	Baltic inflow
River plumes	Adour plume	ADPM	4%	0%	0%	0%	0%	0%	0%	0%	0%	0%	0%	0%	0%	0%	0%	0%	0%	0%	0%	0%	0%	0%	96%	0%
	Elbe plume	ELPM	0%	1%	4%	0%	4%	6%	6%	2%	0%	17%	1%	0%	0%	0%	0%	0%	0%	0%	0%	0%	0%	0%	60%	0%
	Ems plume	EMPM	0%	1%	5%	0%	5%	8%	10%	3%	0%	1%	0%	0%	0%	0%	0%	0%	0%	0%	0%	0%	0%	0%	67%	0%
	Gironde plume	GDPM	2%	6%	0%	0%	0%	0%	0%	0%	0%	0%	0%	0%	0%	0%	0%	0%	0%	0%	0%	0%	0%	0%	92%	0%
	Humber plume	HPM	0%	0%	0%	0%	0%	0%	0%	0%	0%	0%	0%	0%	0%	0%	0%	19%	6%	1%	0%	0%	0%	0%	72%	0%
	Liverpool Bay plume	LBPM	0%	0%	0%	0%	0%	0%	0%	0%	0%	0%	0%	0%	0%	0%	0%	0%	0%	0%	1%	33%	1%	0%	65%	0%
	Loire plume	LPM	2%	4%	0%	0%	0%	0%	0%	0%	0%	0%	0%	0%	0%	0%	0%	0%	0%	0%	0%	0%	0%	0%	94%	0%
	Meuse plume	MPM	0%	1%	8%	0%	10%	11%	0%	0%	0%	0%	0%	0%	0%	0%	0%	0%	0%	0%	0%	0%	0%	0%	70%	0%
	Rhine plume	RHPM	0%	1%	6%	0%	7%	13%	3%	0%	0%	0%	0%	0%	0%	0%	0%	0%	0%	0%	0%	0%	0%	0%	69%	0%
	Scheldt plume 1	SCHPM1	0%	1%	7%	0%	31%	3%	0%	0%	0%	0%	0%	0%	0%	0%	0%	0%	0%	0%	0%	0%	0%	0%	58%	0%
	Scheldt plume 2	SCHPM2	0%	1%	8%	0%	12%	7%	0%	0%	0%	0%	0%	0%	0%	0%	0%	0%	0%	0%	0%	0%	0%	0%	72%	0%
	Shannon plume	SHPM	0%	0%	0%	0%	0%	0%	0%	0%	0%	0%	0%	0%	0%	0%	0%	0%	0%	0%	0%	0%	0%	6%	93%	0%
	Seine plume	SPM	0%	1%	40%	0%	0%	0%	0%	0%	0%	0%	0%	0%	0%	0%	0%	0%	0%	0%	0%	0%	0%	0%	59%	0%
	Thames plume	THPM	0%	1%	0%	2%	0%	0%	0%	0%	0%	0%	0%	0%	0%	0%	8%	2%	1%	0%	0%	0%	0%	0%	84%	0%
Coastal areas	Coastal IRL 3	CIRL	0%	0%	0%	0%	0%	0%	0%	0%	0%	0%	0%	0%	0%	0%	0%	0%	0%	0%	1%	1%	4%	1%	93%	0%
	Coastal NOR 1	CNOR1	0%	0%	0%	0%	0%	0%	0%	0%	0%	0%	0%	0%	0%	0%	0%	0%	0%	0%	0%	0%	0%	0%	95%	1%
	Coastal NOR 2	CNOR2	0%	0%	0%	0%	0%	0%	0%	0%	0%	0%	0%	0%	0%	1%	0%	0%	0%	0%	0%	0%	0%	0%	94%	1%
	Coastal NOR 3	CNOR3	0%	0%	1%	0%	0%	1%	0%	0%	0%	1%	0%	0%	0%	0%	0%	0%	1%	0%	0%	0%	0%	0%	93%	2%
	Outer Coastal DEDK	CO	0%	1%	3%	0%	2%	4%	2%	1%	0%	3%	0%	0%	0%	0%	1%	1%	1%	0%	0%	0%	0%	0%	80%	0%
	Coastal UK 1	CUK1	0%	0%	0%	0%	0%	0%	0%	0%	0%	0%	0%	0%	0%	0%	0%	0%	0%	0%	3%	0%	0%	0%	97%	0%
	Coastal UK channel	CUKC	0%	1%	0%	2%	0%	0%	0%	0%	0%	0%	0%	0%	0%	0%	0%	0%	0%	0%	0%	0%	0%	0%	97%	0%
	East Coast (permanently mixed) 1	ECPM1	0%	0%	0%	0%	0%	0%	0%	0%	0%	0%	0%	0%	0%	0%	0%	0%	0%	1%	0%	1%	0%	0%	97%	0%
	East Coast (permanently mixed) 2	ECPM2	0%	0%	0%	0%	0%	0%	0%	0%	0%	0%	0%	0%	0%	0%	0%	0%	8%	1%	0%	1%	0%	0%	89%	0%
	German Bight central	GBC	0%	1%	4%	0%	3%	5%	2%	0%	0%	1%	0%	0%	0%	0%	1%	0%	0%	0%	0%	0%	0%	0%	81%	0%
	Irish Sea	IRS	0%	0%	0%	0%	0%	0%	0%	0%	0%	0%	0%	0%	0%	0%	0%	0%	0%	0%	2%	3%	1%	0%	92%	0%
	Kattegat Coastal	KC	0%	0%	1%	0%	1%	1%	1%	0%	0%	1%	0%	1%	0%	0%	0%	0%	0%	0%	0%	0%	0%	0%	67%	22%
	Kattegat Deep	KD	0%	0%	1%	0%	1%	2%	1%	0%	0%	2%	0%	0%	0%	0%	1%	0%	1%	0%	0%	0%	0%	0%	78%	10%
	Southern North Sea	SNS	0%	1%	2%	1%	1%	1%	0%	0%	0%	0%	0%	0%	0%	0%	1%	1%	2%	0%	0%	0%	0%	0%	89%	0%
Shelf areas	Atlantic Seasonally Stratified	ASS	0%	1%	2%	1%	0%	0%	0%	0%	0%	0%	0%	0%	0%	0%	0%	0%	0%	0%	0%	0%	0%	0%	95%	0%
	Channel coastal shelf tidal influenced	CFR	0%	1%	14%	0%	0%	0%	0%	0%	0%	0%	0%	0%	0%	0%	0%	0%	0%	0%	0%	0%	0%	0%	84%	0%
	Channel well mixed	CWM	1%	1%	0%	0%	0%	0%	0%	0%	0%	0%	0%	0%	0%	0%	0%	0%	0%	0%	0%	0%	0%	0%	99%	0%
	Channel well mixed tidal influenced	CWMTI	0%	1%	1%	0%	0%	0%	0%	0%	0%	0%	0%	0%	0%	0%	0%	0%	0%	0%	0%	0%	0%	0%	97%	0%
	Dogger Bank	DB	0%	0%	0%	0%	0%	0%	0%	0%	0%	0%	0%	0%	0%	0%	0%	0%	0%	1%	0%	0%	0%	0%	98%	0%
	Eastern North Sea	ENS	0%	0%	0%	0%	0%	0%	0%	0%	0%	0%	0%	0%	0%	0%	1%	1%	1%	1%	0%	0%	0%	0%	94%	0%
	Gulf of Biscay coastal waters	GBCW	2%	3%	0%	0%	0%	0%	0%	0%	0%	0%	0%	0%	0%	0%	0%	0%	0%	0%	0%	0%	0%	0%	95%	0%
	Gulf of Biscay shelf waters	GBSW	1%	1%	0%	0%	0%	0%	0%	0%	0%	0%	0%	0%	0%	0%	0%	0%	0%	0%	0%	0%	0%	0%	98%	0%
	Intermittently Stratified 1	IS1	0%	0%	0%	0%	0%	0%	0%	0%	0%	0%	0%	0%	0%	0%	0%	0%	0%	0%	0%	0%	0%	0%	99%	0%
	Intermittently Stratified 2	IS2	0%	0%	0%	0%	0%	0%	0%	0%	0%	0%	0%	0%	0%	0%	0%	0%	0%	0%	0%	0%	0%	0%	98%	0%
	Northern North Sea	NNS	0%	0%	0%	0%	0%	0%	0%	0%	0%	0%	0%	0%	0%	0%	0%	0%	0%	0%	0%	0%	0%	0%	99%	0%
	Norwegian Trench	NT	0%	0%	0%	0%	0%	0%	0%	0%	0%	0%	0%	0%	0%	0%	0%	0%	0%	0%	0%	0%	0%	0%	98%	0%
	Skagerrak	SK	0%	0%	1%	0%	0%	1%	0%	0%	0%	0%	1%	0%	0%	0%	0%	0%	0%	1%	0%	0%	0%	0%	93%	1%
	Scottish Sea	SS	0%	0%	0%	0%	0%	0%	0%	0%	0%	0%	0%	0%	0%	0%	0%	0%	0%	2%	0%	1%	0%	1%	95%	0%

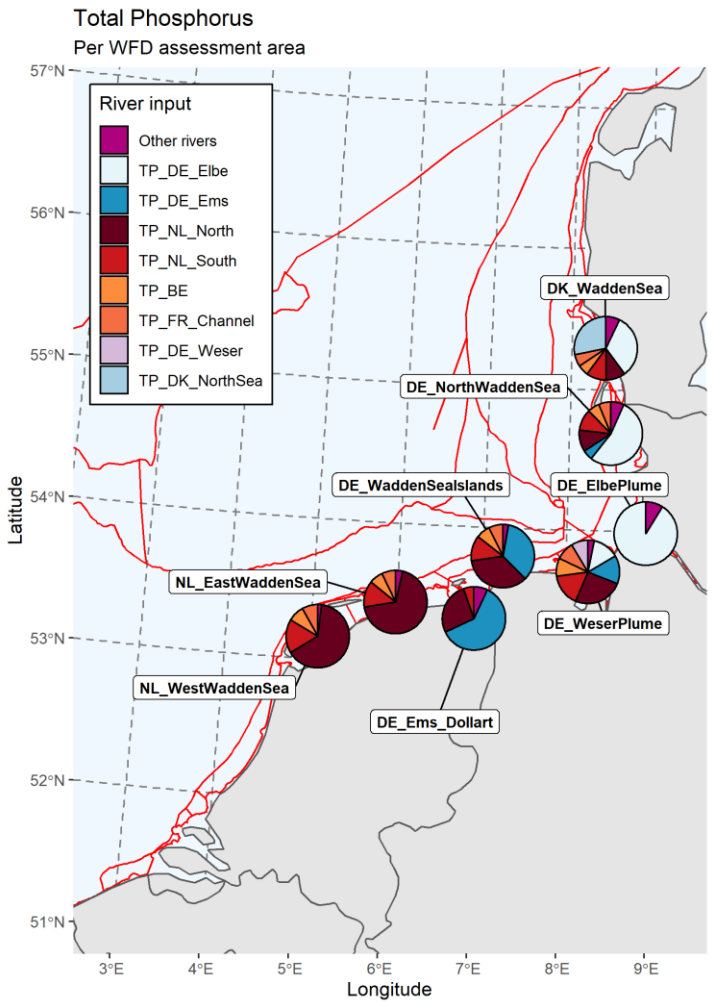

Figure 3-4 Relative contribution of the river sources to the annual mean total-P concentration in the Wadden Sea areas. The pies show the contribution of each river source, with the contribution from the Atlantic Ocean excluded.

Table 3.2 Relative contribution of all sources to the annual mean total-P concentration in parts of the Wadden Sea. Contributions from rivers >5% are highlighted in grey. The contribution from the Atlantic Ocean is highlighted in orange when it is <90%.

Area name	FR_Channel	BE	NL_South	NL_North	DE_Ems	DE_Weser	DE_Elbe	DK_NorthSea	Atlantic Ocean	Other sources
NL west Wadden Sea	4%	4%	**9%**	**33%**	0%	0%	0%	0%	**48%**	1%
NL east Wadden Sea	4%	4%	**7%**	**37%**	1%	0%	0%	0%	**46%**	1%
Ems Dollard	2%	2%	4%	**19%**	**45%**	0%	0%	0%	**27%**	1%
Weser	4%	4%	**7%**	**11%**	**6%**	4%	**6%**	0%	**56%**	1%
DE Wadden Sea islands	4%	4%	**7%**	**18%**	**18%**	0%	0%	0%	**48%**	1%
Elbe	1%	1%	2%	2%	1%	0%	**78%**	0%	**14%**	0%
DE north Wadden Sea	3%	3%	**6%**	**6%**	3%	0%	**28%**	2%	**48%**	1%
DK Wadden Sea	3%	3%	**5%**	**5%**	2%	0%	**17%**	**15%**	**48%**	1%

3.2 Total nitrogen

The tracer model results for nitrogen showed a spatial pattern that was more or less similar to the pattern for phosphorus. The main difference was the generally larger contribution from river sources and the significant contribution of atmospheric deposition. The influence from riverine sources was strongest in the vicinity of the largest river mouths and in the Kattegat/Sound area. The river influence was visible much further offshore than for total P, especially in the Southern North Sea, along the Dutch, German and Danish coasts.

For all sources from Table 2.1, the contribution to the annual mean concentrations of TN was calculated at the scale of the model grid cells. A selection of the maps, focussing on the Greater North Sea, is shown in Figure 3-5. Pie charts with the relative contribution of the sources are shown in Figure 3-6. Figure 3-7 shows the relative contribution of the river sources and atmospheric deposition after exclusion of the contribution of the Atlantic Ocean.

The influence of the Atlantic Ocean dominated offshore areas in the Celtic Seas, the northern part of the North Sea and OSPAR region IV Bay of Biscay and Iberian coast. Along the SE English coast and the continental coast of the North Sea the contribution of the river sources differed between assessment areas, with a gradual change that followed the transport pattern of the residual current. Table 3.3 gives an overview of the relative contribution of each source to the annual mean TN concentration in each assessment area. As was the case for TP, Figure 3.7 and Table 3.3 illustrate the relevance of transboundary transport in many assessment areas in the Greater North Sea.

The river plumes were generally dominated by the contribution from one or several nearby river sources. The coastal assessment areas and some shelf areas had a relatively large contribution from river sources (>10%), generally a mixture from several rivers. The inflow from the Baltic Sea was a substantial source in the Kattegat assessment areas.
The absolute value of atmospheric nitrogen deposition is highest in the Celtic Seas and Greater North Sea and had a major contribution in many assessment areas.

The WFD water bodies in the Wadden Sea showed a large contribution from Rhine/Meuse and Lake IJssel in the Dutch part of the Wadden Sea and the Elbe dominating as source in the eastern part of the German Wadden Sea (Figure 3-8, Table 3.4).

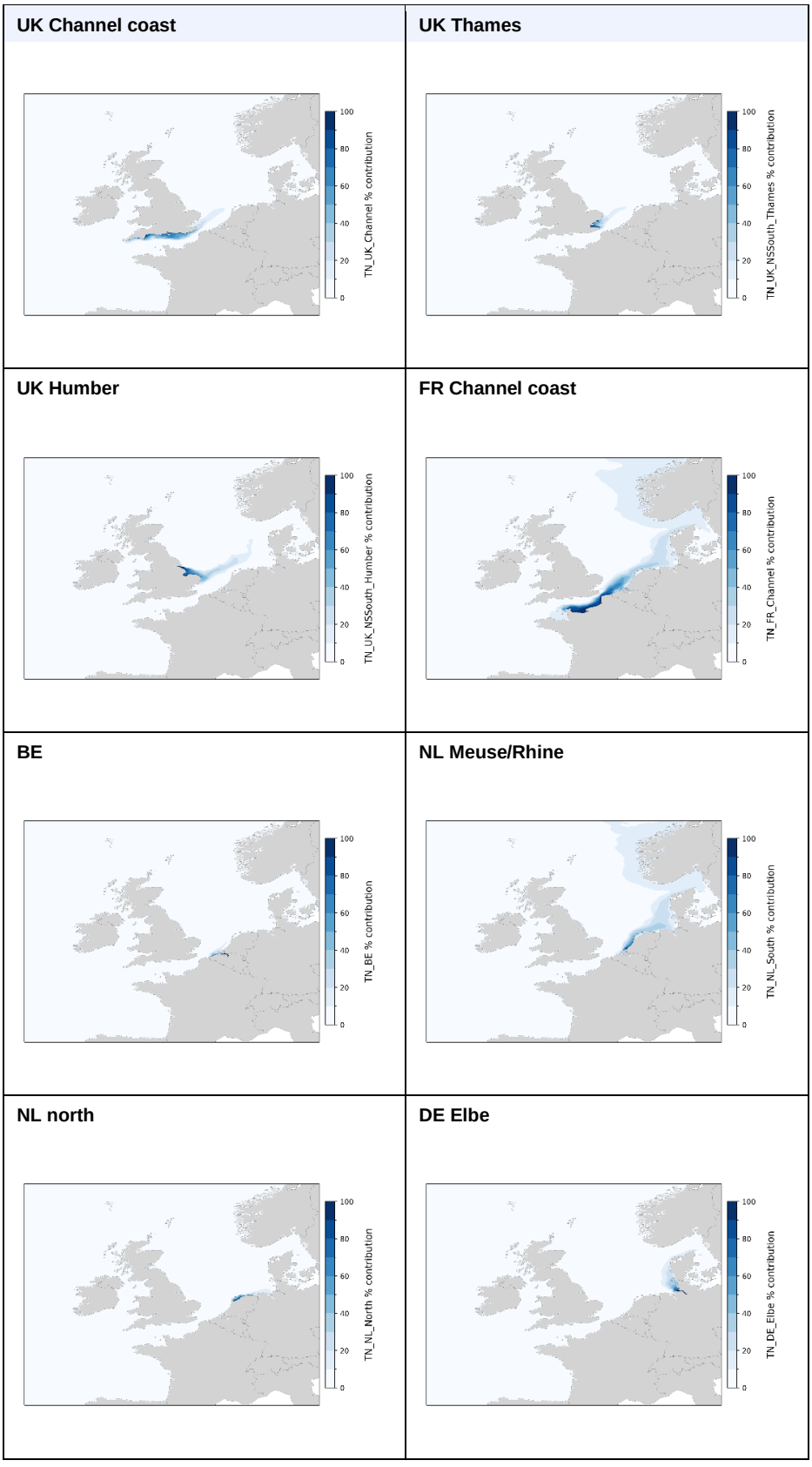

Figure 3-5 Maps showing the relative contribution (in %) of a selection of river sources to the annual mean total-N concentration.

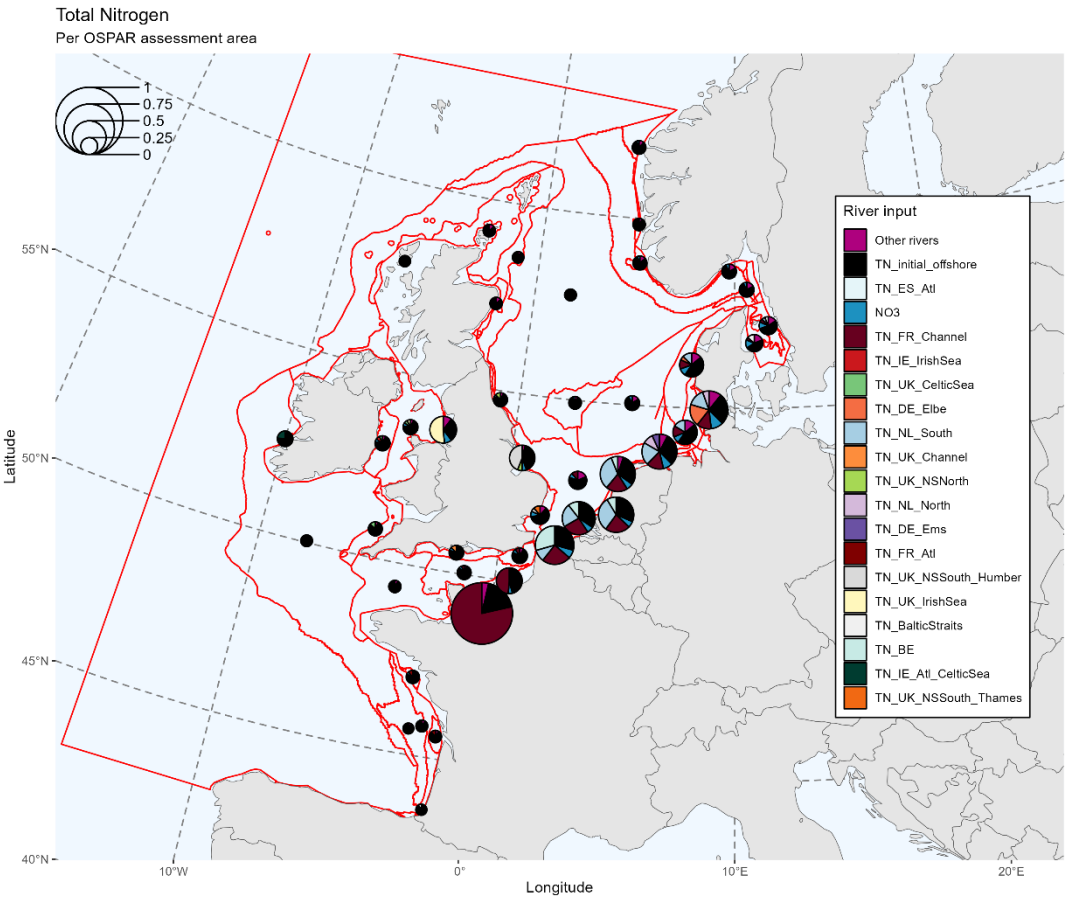

Figure 3-6 Relative contribution of the sources (see Table 2.1) to the annual mean total-N concentration in each COMP4 assessment area. The size of the pie chart indicates the concentration in an assessment area, the pies reflect the contribution of each source. "Other rivers" is the sum of rivers with a contribution to total-N concentration <5%. Atmospheric deposition is labelled 'NO3'.

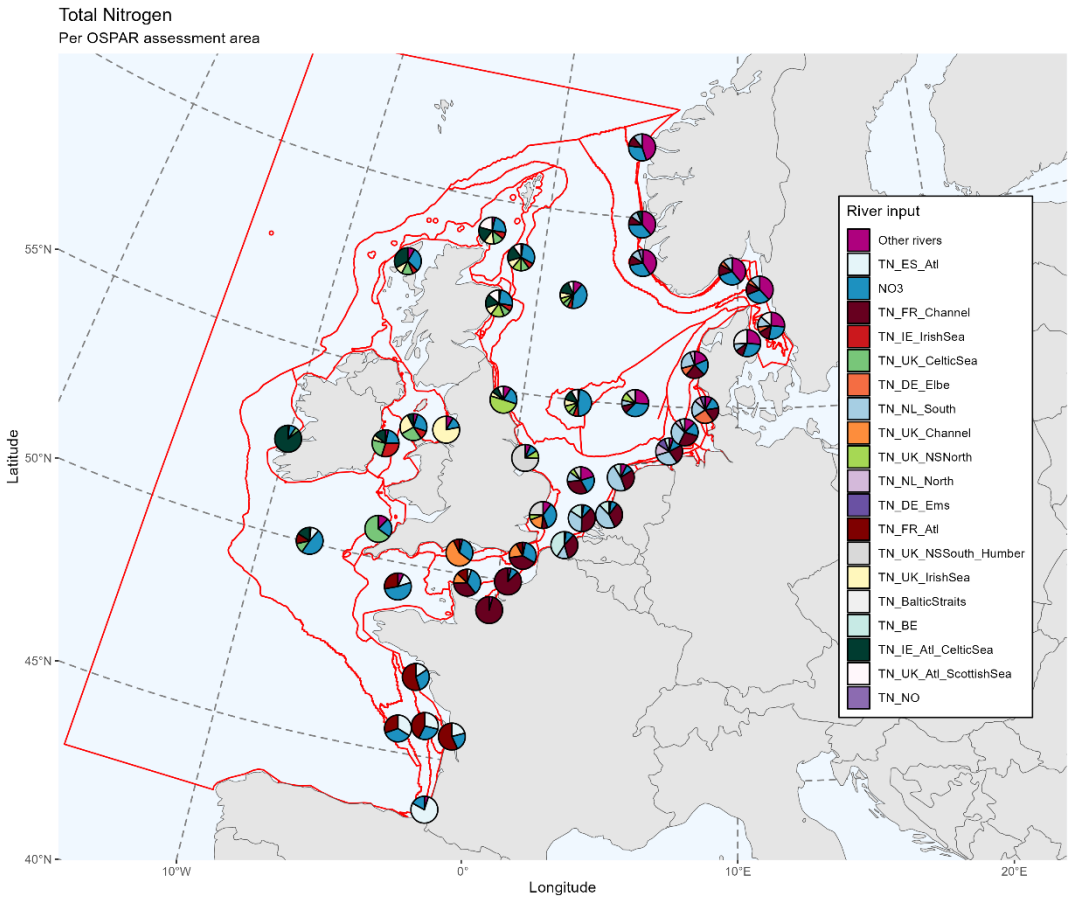

Figure 3-7 Relative contribution of the river sources (see Table 2.1) to the annual mean total-N concentration in each COMP4 assessment area. The pies reflect the contribution of each river source, with the contribution from the Atlantic Ocean excluded. "Other rivers" is the sum of rivers with a contribution to total-N concentration <5%. Atmospheric deposition is labelled 'NO3'.

Table 3.3 Overview of the relative contribution of sources to the TN concentration in each OSPAR assessment area. Contributions from atmospheric deposition or rivers >1% are highlighted in grey. The contribution from the Atlantic Ocean is highlighted in orange when it is <90%.Assessment areas are categorised according to OSPAR (2023).

Category	CPMP4 assessment area name	Area ID	Atm.deposition	ES_Atl	FR_Atl	FR_Channel	UK_Channel	BE	NL_South	NL_North	DE_Ems	DE_Weser	DE_Elbe	DK_NorthSea	DK_Kattegat	SE	NO	UK_Thames	UK_Humber	UK_NorthSeaNorth	UK_Atl_ScottishSea	UK_CelticSea	UK_IrishSea	IE_IrishSea	IE_Atl_CelticSea	Atlantic Ocean	Baltic inflow
River plumes	Adour plume	ADPM	2%	9%	1%	0%	0%	0%	0%	0%	0%	0%	0%	0%	0%	0%	0%	0%	0%	0%	0%	0%	0%	0%	0%	88%	0%
	Elbe plume	ELPM	11%	0%	1%	13%	0%	3%	15%	5%	4%	0%	19%	1%	0%	0%	0%	0%	0%	0%	0%	0%	0%	0%	0%	27%	0%
	Ems plume	EMPM	9%	0%	1%	16%	0%	4%	21%	10%	7%	0%	2%	0%	0%	0%	0%	0%	0%	0%	0%	0%	0%	0%	0%	30%	0%
	Gironde plume	GDPM	5%	4%	12%	0%	0%	0%	0%	0%	0%	0%	0%	0%	0%	0%	0%	0%	0%	0%	0%	0%	0%	0%	0%	79%	0%
	Humber plume	HPM	6%	0%	0%	0%	0%	0%	0%	0%	0%	0%	0%	0%	0%	0%	0%	0%	44%	6%	1%	0%	1%	1%	1%	41%	0%
	Liverpool Bay plume	LBPM	9%	0%	0%	0%	0%	0%	0%	0%	0%	0%	0%	0%	0%	0%	0%	0%	0%	0%	0%	3%	52%	1%	1%	34%	0%
	Loire plume	LPM	6%	3%	12%	0%	0%	0%	0%	0%	0%	0%	0%	0%	0%	0%	0%	0%	0%	0%	0%	0%	0%	0%	0%	79%	0%
	Meuse plume	MPM	6%	0%	1%	23%	0%	9%	31%	0%	0%	0%	0%	0%	0%	0%	0%	0%	0%	0%	0%	0%	0%	0%	0%	30%	0%
	Rhine plume	RHPM	6%	0%	1%	20%	0%	6%	33%	3%	0%	0%	0%	0%	0%	0%	0%	0%	0%	0%	0%	0%	0%	0%	0%	30%	0%
	Scheldt plume 1	SCHPM1	7%	0%	1%	24%	0%	29%	10%	0%	0%	0%	0%	0%	0%	0%	0%	0%	0%	0%	0%	0%	0%	0%	0%	28%	0%
	Scheldt plume 2	SCHPM2	6%	0%	1%	26%	0%	11%	23%	0%	0%	0%	0%	0%	0%	0%	0%	0%	0%	0%	0%	0%	0%	0%	0%	33%	0%
	Shannon plume	SHPM	2%	0%	0%	0%	0%	0%	0%	0%	0%	0%	0%	0%	0%	0%	0%	0%	0%	0%	0%	1%	0%	0%	24%	72%	0%
	Seine plume	SPM	3%	0%	1%	79%	0%	0%	0%	0%	0%	0%	0%	0%	0%	0%	0%	0%	0%	0%	0%	0%	0%	0%	0%	18%	0%
	Thames plume	THPM	10%	0%	1%	2%	5%	0%	0%	0%	0%	0%	0%	0%	0%	0%	0%	11%	7%	2%	0%	0%	0%	0%	0%	60%	0%
Coastal areas	Coastal IRL 3	CIRL	6%	0%	0%	0%	0%	0%	0%	0%	0%	0%	0%	0%	0%	0%	0%	0%	0%	0%	0%	7%	2%	9%	4%	71%	0%
	Coastal NOR 1	CNOR1	6%	0%	0%	2%	0%	0%	2%	0%	0%	0%	1%	0%	0%	0%	1%	0%	1%	1%	0%	0%	0%	0%	1%	82%	1%
	Coastal NOR 2	CNOR2	6%	0%	0%	2%	0%	0%	2%	1%	0%	0%	1%	0%	0%	0%	1%	0%	1%	1%	0%	0%	0%	0%	1%	80%	1%
	Coastal NOR 3	CNOR3	7%	0%	0%	3%	1%	1%	3%	1%	0%	0%	1%	0%	0%	1%	0%	0%	1%	1%	0%	0%	0%	0%	1%	75%	1%
	Outer Coastal DEDK	CO	10%	0%	1%	13%	1%	3%	13%	3%	2%	0%	5%	0%	0%	0%	0%	1%	1%	1%	0%	0%	0%	0%	0%	46%	0%
	Coastal UK 1	CUK1	5%	0%	1%	0%	0%	0%	0%	0%	0%	0%	0%	0%	0%	0%	0%	0%	0%	0%	0%	13%	0%	0%	0%	80%	0%
	Coastal UK channel	CUKC	7%	1%	2%	0%	13%	0%	0%	0%	0%	0%	0%	0%	0%	0%	0%	0%	0%	0%	0%	0%	0%	0%	0%	78%	0%
	East Coast (permanently mixed) 1	ECPM1	4%	0%	0%	0%	0%	0%	0%	0%	0%	0%	0%	0%	0%	0%	0%	0%	0%	2%	2%	1%	1%	1%	2%	86%	0%
	East Coast (permanently mixed) 2	ECPM2	5%	0%	0%	0%	0%	0%	0%	0%	0%	0%	0%	0%	0%	0%	0%	0%	0%	12%	2%	1%	1%	1%	2%	75%	0%
	German Bight central	GBC	9%	0%	1%	15%	1%	3%	16%	3%	1%	0%	1%	0%	0%	0%	0%	1%	1%	1%	0%	0%	0%	0%	0%	45%	0%
	Irish Sea	IRS	7%	0%	0%	0%	0%	0%	0%	0%	0%	0%	0%	0%	0%	0%	0%	0%	0%	0%	0%	8%	8%	3%	2%	71%	0%
	Kattegat Coastal	KC	15%	0%	0%	5%	1%	1%	5%	1%	1%	0%	2%	1%	2%	1%	0%	0%	1%	1%	0%	0%	0%	0%	0%	47%	14%
	Kattegat Deep	KD	12%	0%	1%	6%	1%	1%	6%	2%	1%	0%	3%	1%	1%	1%	0%	1%	1%	1%	0%	0%	0%	0%	0%	54%	6%
	Southern North Sea	SNS	8%	0%	1%	12%	2%	2%	4%	1%	0%	0%	0%	0%	0%	0%	0%	1%	3%	2%	0%	0%	0%	0%	1%	62%	0%
Shelf areas	Atlantic Seasonally Stratified	ASS	2%	0%	1%	0%	0%	0%	0%	0%	0%	0%	0%	0%	0%	0%	0%	0%	0%	0%	0%	0%	0%	0%	1%	96%	0%
	Channel coastal shelf tidal influence	CFR	5%	1%	2%	49%	0%	0%	0%	0%	0%	0%	0%	0%	0%	0%	0%	0%	0%	0%	0%	0%	0%	0%	0%	44%	0%
	Channel well mixed	CWM	5%	1%	2%	0%	0%	0%	0%	0%	0%	0%	0%	0%	0%	0%	0%	0%	0%	0%	0%	0%	0%	0%	0%	91%	0%
	Channel well mixed tidal influenced	CWMTI	6%	1%	2%	6%	2%	0%	0%	0%	0%	0%	0%	0%	0%	0%	0%	0%	0%	0%	0%	0%	0%	0%	0%	82%	0%
	Dogger Bank	DB	6%	0%	0%	0%	0%	0%	0%	0%	0%	0%	0%	0%	0%	0%	0%	0%	0%	1%	1%	1%	1%	1%	2%	87%	0%
	Eastern North Sea	ENS	8%	0%	0%	2%	1%	0%	2%	0%	0%	0%	0%	0%	0%	0%	0%	1%	3%	2%	1%	1%	1%	1%	1%	76%	0%
	Gulf of Biscay coastal waters	GBCW	5%	5%	7%	0%	0%	0%	0%	0%	0%	0%	0%	0%	0%	0%	0%	0%	0%	0%	0%	0%	0%	0%	0%	84%	0%
	Gulf of Biscay shelf waters	GBSW	3%	3%	2%	0%	0%	0%	0%	0%	0%	0%	0%	0%	0%	0%	0%	0%	0%	0%	0%	0%	0%	0%	0%	92%	0%
	Intermittently Stratified 1	IS1	1%	0%	0%	0%	0%	0%	0%	0%	0%	0%	0%	0%	0%	0%	0%	0%	0%	0%	0%	0%	1%	0%	1%	96%	0%
	Intermittently Stratified 2	IS2	2%	0%	0%	0%	0%	0%	0%	0%	0%	0%	0%	0%	0%	0%	0%	0%	0%	1%	1%	1%	1%	0%	1%	93%	0%
	Northern North Sea	NNS	2%	0%	0%	0%	0%	0%	0%	0%	0%	0%	0%	0%	0%	0%	0%	0%	0%	0%	0%	0%	0%	0%	1%	95%	0%
	Norwegian Trench	NT	3%	0%	0%	1%	0%	0%	1%	0%	0%	0%	0%	0%	0%	0%	0%	0%	0%	0%	0%	0%	0%	0%	1%	91%	0%
	Skagerrak	SK	8%	0%	0%	3%	1%	1%	3%	1%	0%	0%	1%	0%	0%	0%	0%	0%	1%	1%	0%	0%	0%	0%	1%	75%	1%
	Scottish Sea	SS	3%	0%	0%	0%	0%	0%	0%	0%	0%	0%	0%	0%	0%	0%	0%	0%	0%	0%	3%	2%	2%	1%	3%	86%	0%

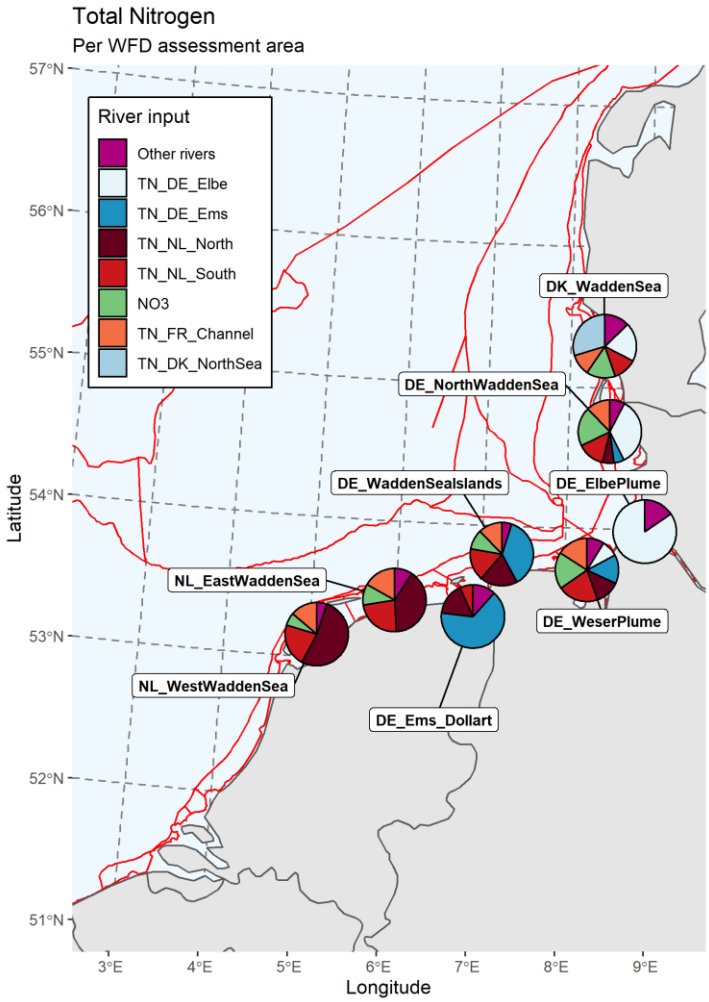

Figure 3-8 Relative contribution of the river sources to the annual mean total-N concentration in the Wadden Sea areas. The pies show the contribution of each river source, with the contribution from the Atlantic Ocean excluded.

Table 3.4 Relative contribution of all sources to the annual mean total-N concentration in parts of the Wadden Sea. Contributions from rivers >5% are highlighted in grey. The contribution from the Atlantic Ocean is highlighted in orange when it is <90%.

Area name	Atm.dep.	FR_Channel	BE	NL_South	NL_North	DE_Ems	DE_Weser	DE_Elbe	DK_NorthSea	Atlantic Ocean	Other sources
NL west Wadden Sea	**5%**	**11%**	3%	**18%**	**43%**	0%	0%	0%	0%	**18%**	0%
NL east Wadden Sea	**8%**	**13%**	4%	**18%**	**31%**	2%	0%	0%	0%	**22%**	1%
Ems Dollard	5%	4%	1%	**6%**	**15%**	**60%**	0%	0%	0%	**8%**	0%
Weser	**14%**	**12%**	3%	**16%**	**10%**	**11%**	2%	**6%**	0%	**23%**	1%
DE Wadden Sea islands	**8%**	**10%**	3%	**14%**	**16%**	**31%**	0%	0%	0%	**18%**	1%
Elbe	4%	3%	1%	3%	2%	2%	0%	**80%**	0%	**5%**	0%
DE north Wadden Sea	**16%**	**10%**	2%	**11%**	5%	4%	0%	**28%**	2%	**19%**	1%
DK Wadden Sea	**12%**	**9%**	2%	**10%**	4%	3%	0%	**16%**	**24%**	**18%**	1%

3.3 Conclusions

The results of the tracer modelling showed similar patterns as the results from earlier tracer studies. The offshore areas were mostly dominated by the influence of the Atlantic Ocean. The highest contributions of riverine loads were found near the mouths of the largest rivers, along the Channel's coasts, the southern North Sea and the Skagerrak/Kattegat.
For nitrogen, the riverine contribution was relatively high compared to phosphorus, which can partly be explained by the fact that riverine P-loads have decreased more strongly than N-loads in the last decades and, consequently, the relative contribution of inputs from the Atlantic Ocean is higher for P. This is also supported by the increase in observed N:P ratios in the total loads (waterborne+airborne) to the Greater North Sea, Celtic Seas and Bay of Biscay and Iberian coast (Axe *et al.* 2023). Also, nitrogen concentrations decrease in marine waters due to denitrification, which leads to naturally steeper gradients in nitrogen concentrations from freshwater to marine waters, compared to phosphorus.
For nitrogen, atmospheric deposition had a substantial contribution in all assessment areas except remote oceanic areas.

4 Model validation with current state (2015-2017) results

4.1 Time series

Model results from the present study for 2015-2017 showed that compared to the previously reported OSPAR runs (Lenhart *et al.* 2022), the recent model upgrade (as described in Section 2.6) led to a slight decrease in winter nutrient concentrations and in growing season chlorophyll-a concentrations at MWTL stations, better matching observed concentrations: both at a nearshore location (NOORDWK20, situated 20 km off the Dutch coast in the Rhine plume (Figure 4-1)) and an offshore location (TERSLG235 in the assessment area Dogger Bank (Figure 4-2)).

Satellite observations were overall consistent with MWTL measurement time-series and provided more frequent observations for model validation. By comparing our model results to the OSPAR satellite data, we could see that the model captured the timing of the spring bloom well. At the near-shore NOORDWK20 station, some chlorophyll peaks in the middle of the growing season were not captured. At TERSLG235, chlorophyll-a concentrations were overestimated by the model throughout the growing season, but particularly during the spring bloom, and declined too early in autumn, compared to the observations.

Concentrations of phosphate and, to a lesser extent, DIN were underestimated in the summer period.

4.2 Spatial patterns

Maps of the model results were used to compare the spatial patterns in model results and observations. This comparison was made for the 2015-2017 average of the winter means of DIP (Figure 4-3), DIN (Figure 4-4) and the growing season mean of chlorophyll (Figure 4-5). For chlorophyll, model results were also compared to satellite data for the years 2015 (Figure 4-6), 2016 (Figure 4-7) and 2017 (Figure 4-8).

These results showed that the model captured spatial gradients in winter nutrient concentrations well, from higher concentrations nearshore to lower concentrations in more offshore areas. Spatial gradients of growing season chlorophyll-a concentrations were well captured along the coasts. The model however still overestimated chlorophyll concentrations further offshore and in the Skagerrak/Kattegat areas.

This was confirmed by comparing model results with satellite observations. While satellite data showed growing season chlorophyll concentrations <2 µg/L over a large part of the domain, the model did not capture these very low offshore concentrations and provided concentrations of 2-4 µg/L in most offshore areas. The model results were lower than satellite estimates along the Belgian coast and in the entire Wadden Sea, as well as along UK coasts and in the Thames plume. This may also have been due to overestimation of chlorophyll-a in the satellite data of these very turbid waters. High turbidity is known to negatively affect the reliability of the retrieval of chlorophyll-a concentrations in satellite data. The model did capture interannual variability, with highest offshore concentrations in 2015 and lowest in 2017.

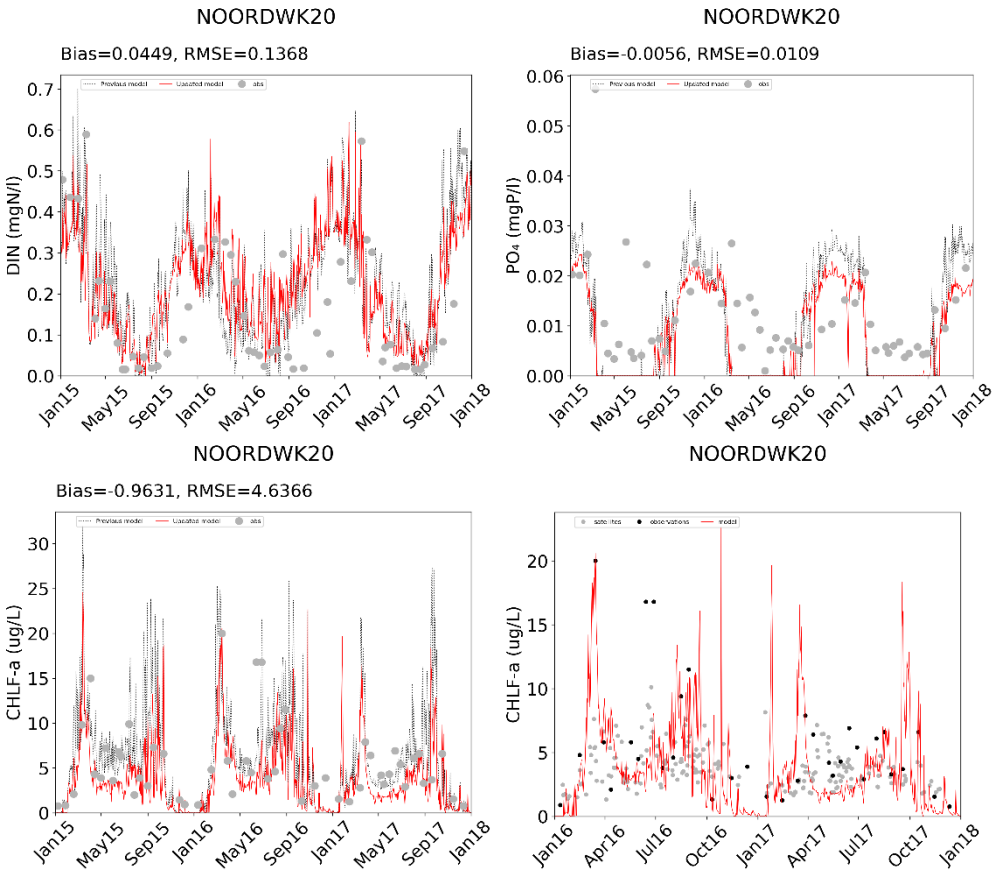

Figure 4-1 Timeseries of model results after model improvement (red line) compared with previous model results (grey/dotted line) and observations for station Noordwijk 20. In the upper panels and bottom-left panel grey dots are MWTL (in situ) measurements. In the bottom-right panel grey dots are observations extracted from satellite data and black dots are MWTL (in situ) observations.

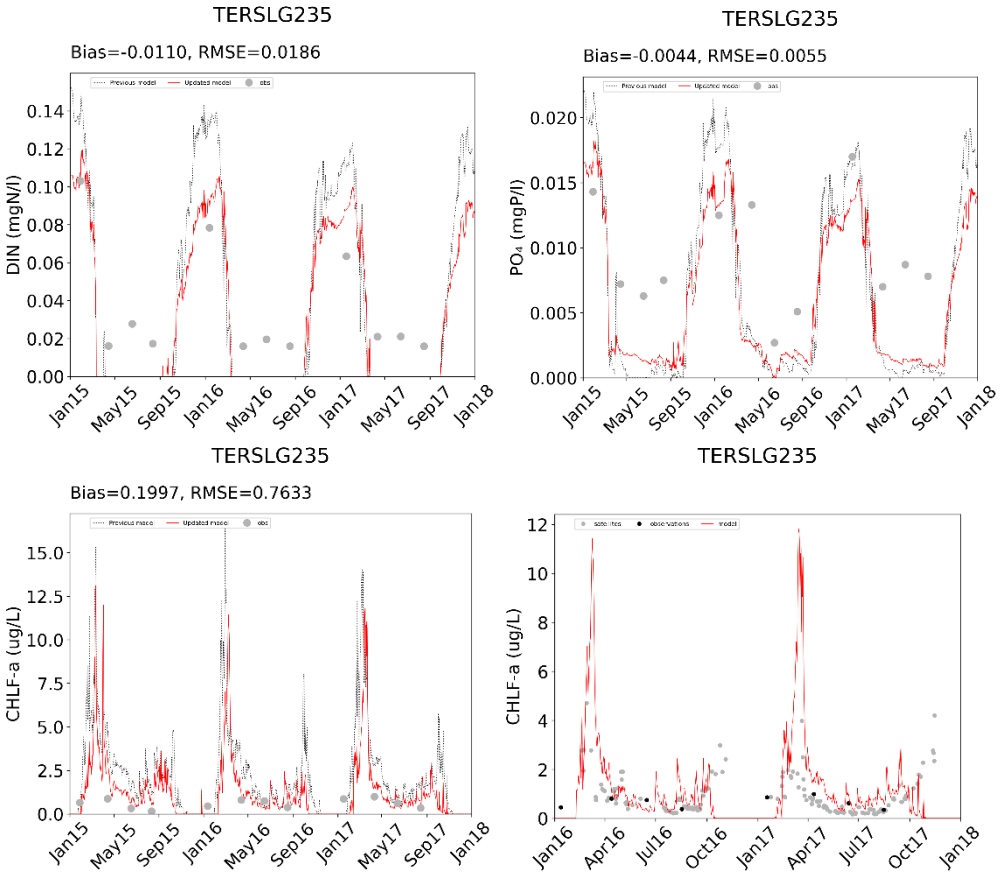

Figure 4-2 Timeseries of model results after model improvement (red line) compared with previous model results (grey line) and observations for station Terschelling 235. In the upper panels and bottom-left panel grey dots are MWTL (in situ) measurements. In the bottom-right panel grey dots are observations extracted from satellite data and black dots are MWTL (in situ) observations.

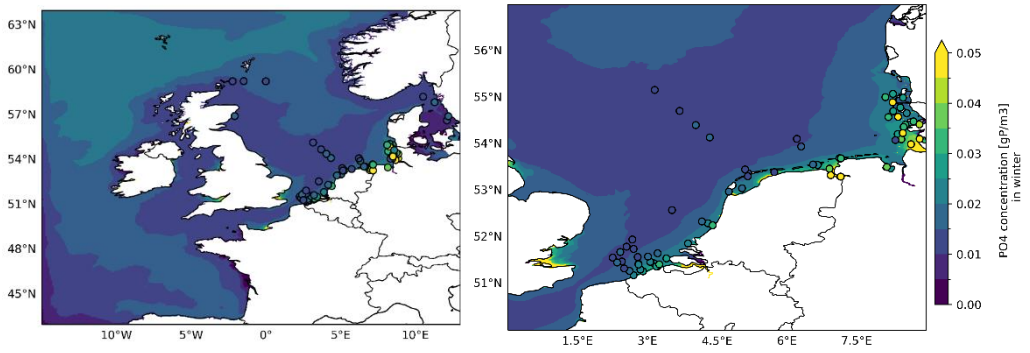

Figure 4-3 Maps of modelled winter means of DIP over 2015-2017 and observed concentrations (dots), for the entire model domain (left panel) and zoomed-in at the southern North Sea (right panel).

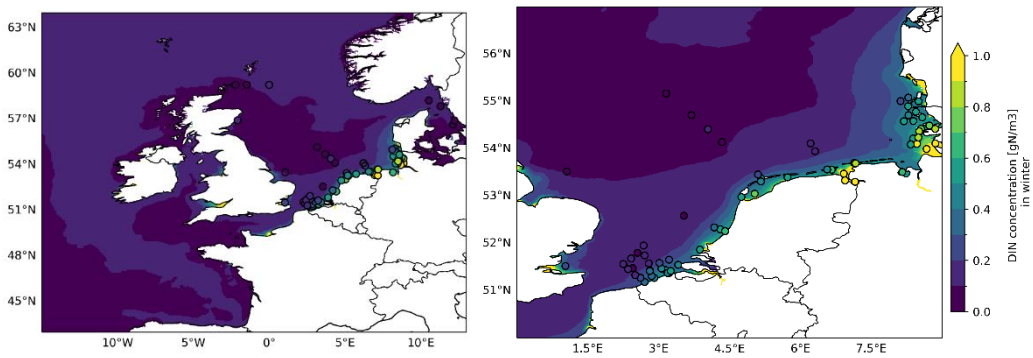

Figure 4-4 Maps of modelled winter means of DIN over 2015-2017 and observed concentrations (dots), for the entire model domain (left panel) and zoomed-in at the southern North Sea (right panel).

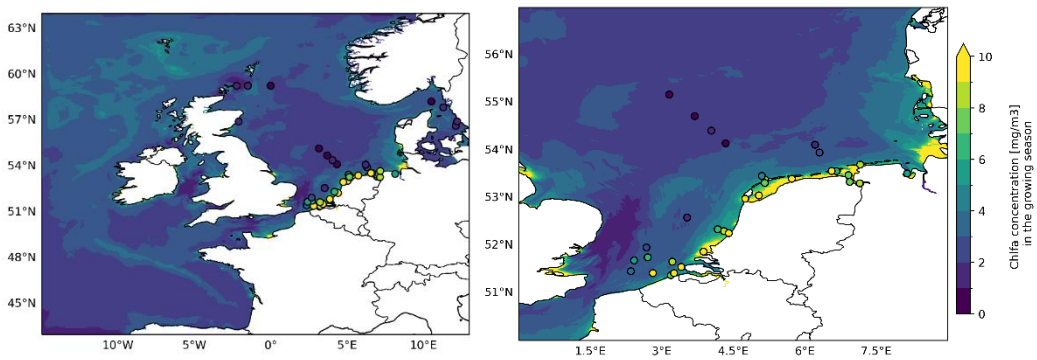

Figure 4-5 Maps of modelled growing season means of chlorophyll over 2015-2017 and observed concentrations (dots), for the entire model domain (left panel) and zoomed-in at the southern North Sea (right panel).

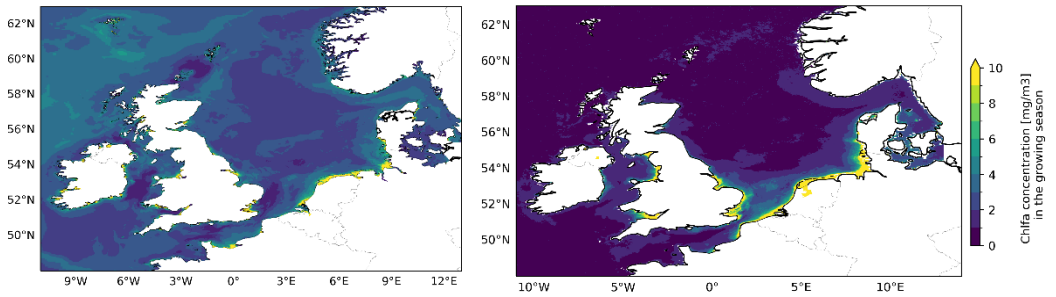

Figure 4-6 Growing season mean (March-October) chlorophyll concentrations from model results (left panel) and satellite observations (right panel) in 2015.

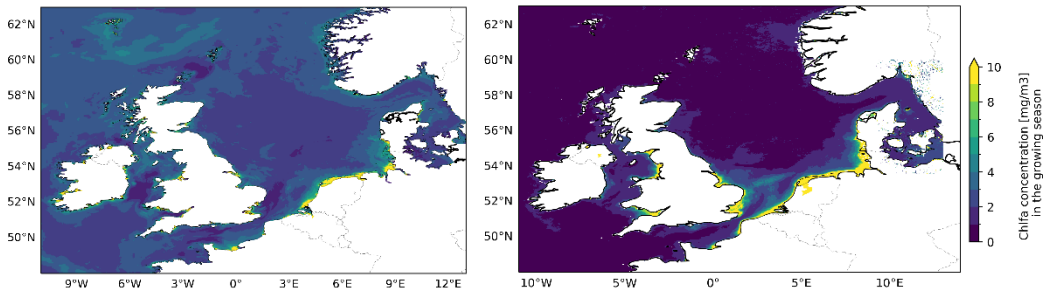

Figure 4-7 Growing season mean (March-October) chlorophyll concentrations from model results (left panel) and satellite observations (right panel) in 2016.

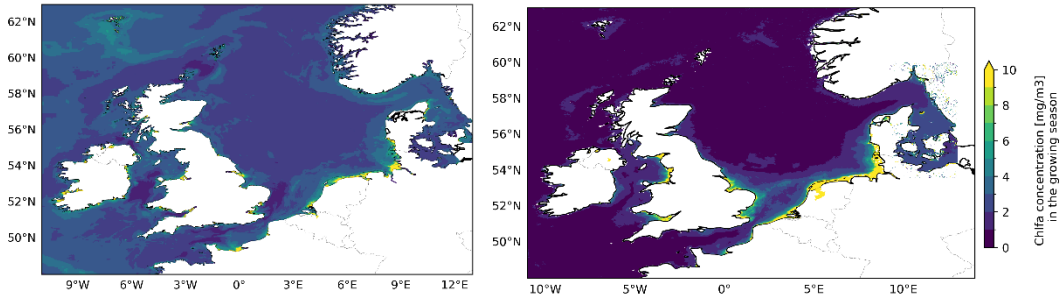

Figure 4-8 Growing season mean (March-October) chlorophyll concentrations from model results (left panel) and satellite observations (right panel) in 2017.

5 Model results of the HS2+50% scenario

5.1 Differences in concentrations between the HS2+50% and current state scenarios

5.1.1 Difference maps

The results of the model scenario with reduced nutrient loads (scenario HS2+50%; see §2.4) are shown in comparison to the current state simulations. Maps with the reduction in concentrations in the HS2+50% scenario compared to current state are shown for DIP (Figure 5-1), DIN (Figure 5-2) and chlorophyll (Figure 5-3).

The maps show that the reduced nutrient scenario HS2+50%, in comparison with the current state, resulted in lower concentrations in some near coastal areas, in the Kattegat, North Sea and parts of the Celtic Seas. In the Kattegat, particularly the DIP concentrations were strongly reduced (over 50%) in the scenario run.

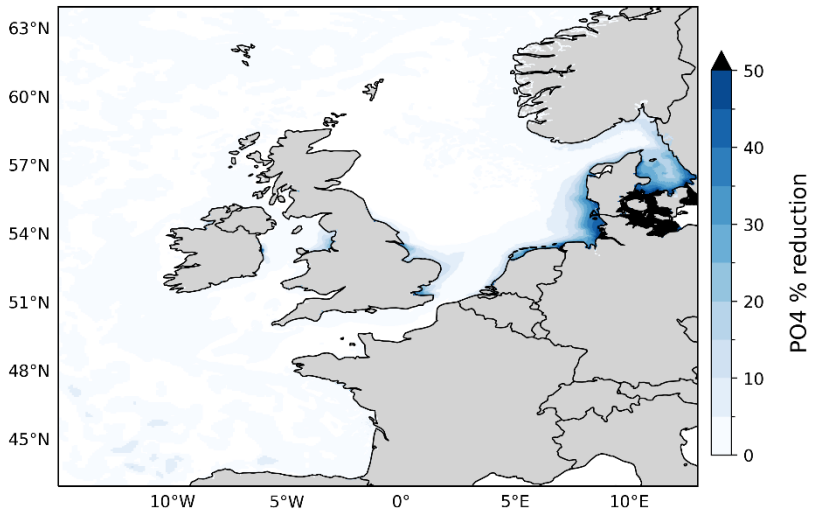

Figure 5-1 Map showing the difference (in %) in winter mean DIP concentrations between the nutrient reduction scenario HS2+50% and the current state run. Results for the model years 2015-2017.

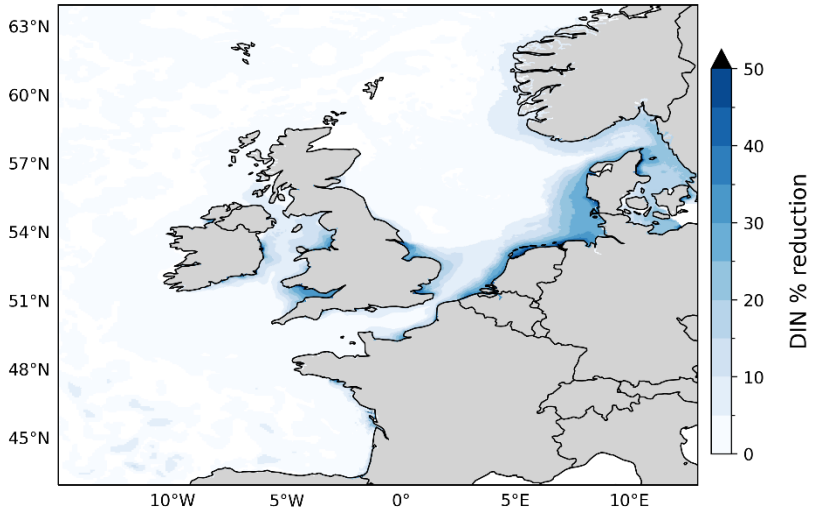

Figure 5-2 Map showing the difference (in %) in winter mean DIN concentrations between the nutrient reduction scenario HS2+50% and the current state run. Results for the model years 2015-2017.

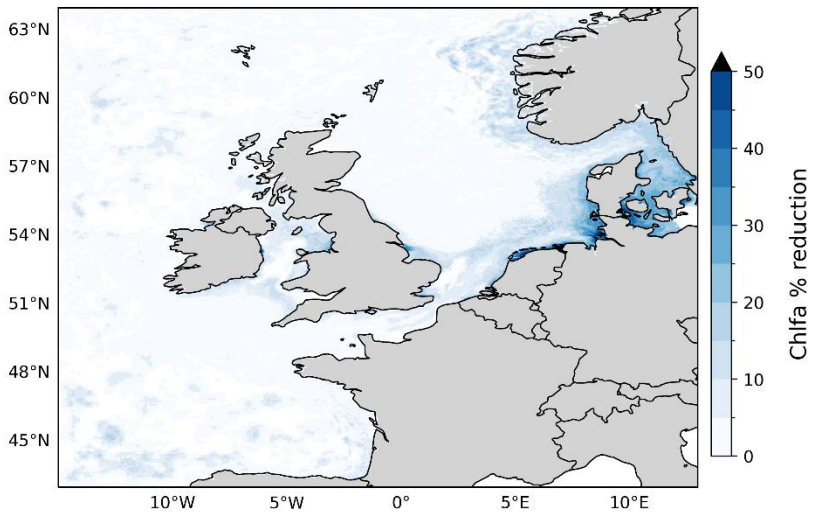

Figure 5-3 Map showing the difference (in %) in growing season mean chlorophyll between the nutrient reduction scenario HS2+50% and the current state run. Results for the model years 2015-2017.

5.1.2 Concentrations of nutrients and chlorophyll in the assessment areas

The winter mean concentrations of DIN, DIP and growing season mean concentrations of chlorophyll in the current state simulation and in the HS2+50% scenario, were calculated for each assessment area, averaged over the years 2015-2017. The concentrations were compared to the thresholds and concentrations from the latest OSPAR assessment (COMP4, OSPAR 2023). Table 5.1 shows the results for DIP, Table 5.2 for DIN and Table 5.3 for chlorophyll. In the latter table, the chlorophyll concentrations from COMP4 calculated by merging *in situ* data and satellite data, were used. The assessment areas are distinguished in four categories: river plumes, coastal areas, shelf areas and oceanic areas, according to OSPAR (2022).

The COMP4 eutrophication assessment (OSPAR 2023) determined in which assessment areas concentrations of DIN, DIP and chlorophyll exceeded the thresholds. Based on that exceedance, we calculated the percentage reduction in concentrations required to achieve non-eutrophication status. From the model runs we calculated the percentage reduction that was achieved in the HS2+50% scenario (compared to the current state simulation). The modelled reductions in scenario HS2+50% were compared to the required reduction following the COMP4 assessment. Obviously, the reduced nutrient loads in the HS2+50% scenario resulted in lower concentrations of DIP, DIN and chlorophyll in the river plumes and coastal assessment areas. The effects in the shelf areas where river influence is generally less, were small with exception of the Skagerrak.

For the assessment areas where concentrations exceeded the threshold in the COMP4 assessment, the reduction that was predicted by the model scenario HS2+50% was, in many cases, sufficient or nearly sufficient to meet the required reduction following from the COMP4 assessment. The largest gaps for DIN, where the required reduction was much larger than the predicted reduction, were found in the Elbe plume and Shannon plume (Table 5.2). For chlorophyll, this was the case for Scheldt and Meuse plume, coastal FR Channel and Kattegat coastal area (Table 5.3)

In the Seine plume, increases were predicted for DIP and chlorophyll in the HS2+50% scenario. This was caused by the higher DIP loads in this scenario, compared to current loads (see Figure 2-4, Table 2.2). The same applies to DIP concentrations in the Shannon plume.

Table 5.1 Thresholds and observed concentrations of DIP (in µM) used in the COMP4 assessment and concentrations from the model scenarios. In those cases where observed concentrations are higher than the COMP4 threshold, a required reduction (in %) was calculated. From the model results the reduction realised in the HS2+50% scenario compared to the current state was calculated.
Green cells: modelled reduction in the HS2+50% scenario >5% larger than the required reduction. Orange cells: modelled reduction in the HS2+50% scenario >5% smaller than the required reduction. Grey cells: Difference between modelled reduction and required reduction <5%. Empty cells indicate missing data and no COMP4 assessment result.

Category	OSPAR region	Assessment area	Code	COMP4			model scenarios		
				Threshold	Concentration (µM)	Reduction required (%)	Current state	HS2+50%	Reduction realised
Plume	IV	Adour plume	ADPM	0,67			0,50	0,48	4%
Plume	II	Elbe plume	ELPM	0,72	0,80	11%	0,70	0,50	28%
Plume	II	Ems plume	EMPM	0,61	0,58		0,71	0,56	21%
Plume	IV	Gironde plume	GDPM	0,68			0,16	0,16	1%
Plume	II	Humber plume	HPM	1,16	0,68		0,63	0,51	19%
Plume	III	Liverpool Bay plume	LBPM	1,35			0,76	0,61	20%
Plume	IV	Loire plume	LPM	0,79			0,40	0,40	1%
Plume	II	Meuse plume	MPM	1,35	0,77		0,71	0,63	12%
Plume	II	Rhine plume	RHPM	1,15	0,94		0,68	0,59	14%
Plume	II	Scheldt plume 1	SCHPM1	1,31	0,91		0,88	0,82	6%
Plume	II	Scheldt plume 2	SCHPM2	1,02	0,10		0,68	0,63	8%
Plume	III	Shannon plume	SHPM	0,84	0,59		0,45	0,47	-3%
Plume	II	Seine plume	SPM	0,91	0,75		1,12	1,16	-4%
Plume	II	Thames plume	THPM	1,04	0,82		0,68	0,59	12%
Coastal	II	Coastal FR channel	CFR	0,60	0,65	7%	0,63	0,64	-2%
Coastal	III	Coastal IRL 3	CIRL	0,77	0,62		0,50	0,48	4%
Coastal	II	Coastal NOR 1	CNOR1	0,87			0,46	0,46	2%
Coastal	II	Coastal NOR 2	CNOR2	0,77			0,45	0,43	5%
Coastal	II	Coastal NOR 3	CNOR3	0,68	0,53		0,39	0,36	8%
Coastal	III	Coastal UK 1	CUK1	0,82	0,47		0,44	0,44	0%
Coastal	II	Coastal UK channel	CUKC	0,73	0,47		0,47	0,46	1%
Coastal	II	East Coast (permanently mixed) 1	ECPM1	0,78	0,57		0,40	0,41	-2%
Coastal	II	East Coast (permanently mixed) 2	ECPM2	0,86	0,55		0,48	0,45	7%
Coastal	II	German Bight (deep)	GBC	0,62	0,54		0,54	0,49	10%
Coastal	III	Irish Sea	IRS	0,78	0,65		0,45	0,44	3%
Coastal	II	Kattegat Coastal	KC	0,45	0,51	11%	0,30	0,22	25%
Coastal	II	Kattegat Deep	KD	0,48	0,51	5%	0,33	0,27	20%
Coastal	II	Outer coastal DEDK	OC DEDK	0,59	0,49		0,54	0,47	13%
Coastal	II	Southern North Sea	SNS	0,70	0,52		0,49	0,47	4%
Shelf	III, IV	Atlantic Seasonally Stratified	ASS	0,84	0,51		0,49	0,49	0%
Shelf	II	Channel coastal shelf tidal	CCTI	0,64	0,50		0,49	0,49	0%
Shelf	II, III	Channel well mixed	CWM	0,66	0,39		0,42	0,42	0%
Shelf	II	Channel well mixed tidal influenced	CWMTI	0,69	0,47		0,46	0,46	0%
Shelf	II	Dogger Bank	DB	0,76	0,49		0,42	0,43	-1%
Shelf	II	Eastern North Sea	ENS	0,60	0,47		0,43	0,42	2%
Shelf	IV	Gulf of Biscay coastal waters	GBCW	0,75			0,36	0,36	1%
Shelf	IV	Gulf of Biscay shelf waters	GBSW	0,69			0,45	0,45	0%
Shelf	II, III	Intermittently Stratified 1	IS1	0,90	0,52		0,53	0,53	0%
Shelf	II	Intermittently Stratified 2	IS2	0,86	0,54		0,45	0,45	-1%
Shelf	II	Northern North Sea	NNS	0,71	0,53		0,48	0,48	0%
Shelf	II	Norwegian Trench	NT	0,60	0,46		0,52	0,51	2%
Shelf	II	Skagerak	SK	0,64	0,50		0,40	0,36	11%
Shelf	II, III	Scottish Sea	SS	0,80	0,54		0,46	0,46	0%

Table 5.2 Thresholds and observed concentrations of DIN (in µM) used in the COMP4 assessment and concentrations from the model scenarios. In those cases where observed concentrations are higher than the COMP4 threshold, a required reduction (in %) was calculated. From the model results the reduction realised in the HS2+50% scenario compared to the current state was calculated.
Green cells: modelled reduction in the HS2+50% scenario >5% larger than the required reduction. Orange cells: modelled reduction in the HS2+50% scenario >5% smaller than the required reduction. Grey cells: Difference between modelled reduction and required reduction <5%. Empty cells indicate missing data and no COMP4 assessment result.

Category	OSPAR region	Assessment area	Code	COMP4			model scenarios		
				Threshold	Concentration (µM)	Reduction required (%)	Current state	HS2+50%	Reduction realised
Plume	IV	Adour plume	ADPM	8,9			8,4	7,2	15%
Plume	II	Elbe plume	ELPM	18,2	28,99	37%	26,2	18,9	**28%**
Plume	II	Ems plume	EMPM	15,1	22,54	33%	25,9	17,6	32%
Plume	IV	Gironde plume	GDPM	12,7			3,0	2,7	10%
Plume	II	Humber plume	HPM	26,3	11,91		19,8	13,8	30%
Plume	III	Liverpool Bay plume	LBPM	22,2			25,5	18,1	29%
Plume	IV	Loire plume	LPM	19,3			6,6	6,3	5%
Plume	II	Meuse plume	MPM	40,7	45,75	11%	38,3	25,6	33%
Plume	II	Rhine plume	RHPM	29,7	41,01	28%	30,7	21,3	30%
Plume	II	Scheldt plume 1	SCHPM1	25,9	34,73	25%	31,1	20,7	33%
Plume	II	Scheldt plume 2	SCHPM2	33,3	7,99		29,4	20,4	31%
Plume	III	Shannon plume	SHPM	11,7	14,97	22%	12,0	12,4	-3%
Plume	II	Seine plume	SPM	27,3	28,36	4%	68,1	51,6	24%
Plume	II	Thames plume	THPM	16,9	15,81		15,1	12,1	20%
Coastal	II	Coastal FR channel	CFR	15,8	15,82	0%	18,7	16,0	14%
Coastal	III	Coastal IRL 3	CIRL	11,4	9,61		10,5	8,8	16%
Coastal	II	Coastal NOR 1	CNOR1	12,5			7,6	7,1	6%
Coastal	II	Coastal NOR 2	CNOR2	10,3			8,4	7,4	13%
Coastal	II	Coastal NOR 3	CNOR3	9,2	8,16		8,7	7,2	17%
Coastal	III	Coastal UK 1	CUK1	11,7	7,05		9,0	7,7	14%
Coastal	II	Coastal UK channel	CUKC	12,8	7,52		9,1	8,3	9%
Coastal	II	East Coast (permanently mixed) 1	ECPM1	11,0	7,51		6,1	6,1	0%
Coastal	II	East Coast (permanently mixed) 2	ECPM2	10,9	6,64		7,8	6,9	11%
Coastal	II	German Bight (deep)	GBC	10,1	13,68	26%	15,2	11,8	22%
Coastal	III	Irish Sea	IRS	9,9	7,81		9,3	8,0	13%
Coastal	II	Kattegat Coastal	KC	4,5	5,98	25%	7,2	5,7	21%
Coastal	II	Kattegat Deep	KD	4,0	5,40	26%	8,4	6,5	22%
Coastal	II	Outer coastal DEDK	OC DEDK	9,3	10,48	11%	16,0	12,2	24%
Coastal	II	Southern North Sea	SNS	13,0	12,39		11,0	9,3	15%
Shelf	III, IV	Atlantic Seasonally Stratified	ASS	11,7	8,62		7,3	7,2	2%
Shelf	II	Channel coastal shelf tidal	CCTI	12,0	9,03		9,7	8,9	8%
Shelf	II, III	Channel well mixed	CWM	8,3	4,26		6,3	6,2	1%
Shelf	II	Channel well mixed tidal influenced	CWMTI	9,2	8,20		7,8	7,5	4%
Shelf	II	Dogger Bank	DB	7,2	5,58		6,1	6,1	0%
Shelf	II	Eastern North Sea	ENS	7,3	5,61		7,8	7,2	7%
Shelf	IV	Gulf of Biscay coastal waters	GBCW	11,8			5,7	5,4	5%
Shelf	IV	Gulf of Biscay shelf waters	GBSW	8,7			6,7	6,6	2%
Shelf	II, III	Intermittently Stratified 1	IS1	13,7	8,04		7,6	7,6	0%
Shelf	II	Intermittently Stratified 2	IS2	11,3	7,41		6,5	6,5	0%
Shelf	II	Northern North Sea	NNS	10,3	7,01		7,0	6,9	1%
Shelf	II	Norwegian Trench	NT	6,6	5,02		8,5	8,0	6%
Shelf	II	Skagerak	SK	4,7	6,01	22%	9,7	7,8	19%
Shelf	II, III	Scottish Sea	SS	9,7	6,72		6,8	6,7	2%

Table 5.3 Thresholds and observed concentrations of chlorophyll (in µg/l) used in the COMP4 assessment and concentrations from the model scenarios. In those cases where observed concentrations are higher than the COMP4 threshold, a required reduction (in %) was calculated. From the model results the reduction realised in the HS2+50% scenario compared to the current state was calculated.
Green cells: modelled reduction in the HS2+50% scenario >5% larger than the required reduction. Orange cells: modelled reduction in the HS2+50% scenario >5% smaller than the required reduction. Grey cells: Difference between modelled reduction and required reduction <5%. Empty cells indicate missing data and no COMP4 assessment result.

Category	OSPAR region	Assessment area	Code	COMP4			model scenarios		
				Threshold	Concentration (µg/l)	Reduction required (%)	Current state	HS2+50%	Reduction realised
Plume	IV	Adour plume	ADPM	1,7	1,54		2,34	2,08	11%
Plume	II	Elbe plume	ELPM	3,7	5,23	29%	4,08	3,04	25%
Plume	II	Ems plume	EMPM	3,7	4,93	25%	4,02	3,17	21%
Plume	IV	Gironde plume	GDPM	5,4	2,26		3,36	3,24	4%
Plume	II	Humber plume	HPM	10,6	6,69		4,38	3,34	24%
Plume	III	Liverpool Bay plume	LBPM	9,0	6,74		5,11	4,01	22%
Plume	IV	Loire plume	LPM	3,3	2,73		2,74	2,64	4%
Plume	II	Meuse plume	MPM	8,0	11,93	33%	10,83	8,66	20%
Plume	II	Rhine plume	RHPM	6,8	7,60	11%	5,87	4,74	19%
Plume	II	Scheldt plume 1	SCHPM1	5,0	12,19	59%	4,38	3,84	12%
Plume	II	Scheldt plume 2	SCHPM2	8,9	11,01	19%	7,68	6,75	12%
Plume	III	Shannon plume	SHPM	1,8	1,33		3,62	3,61	0%
Plume	II	Seine plume	SPM	5,1	3,56		9,31	10,31	-11%
Plume	II	Thames plume	THPM	7,4	5,02		1,87	1,66	11%
Coastal	II	Coastal FR channel	CFR	2,8	3,38	17%	4,24	4,22	0%
Coastal	III	Coastal IRL 3	CIRL	1,8	1,56		2,76	2,55	7%
Coastal	II	Coastal NOR 1	CNOR1	2,7	0,83		2,57	2,35	9%
Coastal	II	Coastal NOR 2	CNOR2	1,9	1,00		3,75	3,30	12%
Coastal	II	Coastal NOR 3	CNOR3	2,4	1,64		3,11	2,68	14%
Coastal	III	Coastal UK 1	CUK1	1,7	1,29		2,68	2,58	4%
Coastal	II	Coastal UK channel	CUKC	2,3	1,46		2,47	2,32	6%
Coastal	II	East Coast (permanently mixed) 1	ECPM1	2,1	1,23		2,69	2,69	0%
Coastal	II	East Coast (permanently mixed) 2	ECPM2	3,5	2,09		3,44	2,99	13%
Coastal	II	German Bight (deep)	GBC	1,9	2,03	7%	2,39	2,07	13%
Coastal	III	Irish Sea	IRS	2,0	1,40		2,65	2,41	9%
Coastal	II	Kattegat Coastal	KC	1,2	1,98	39%	2,46	1,94	21%
Coastal	II	Kattegat Deep	KD	1,4	1,67	16%	2,50	2,01	20%
Coastal	II	Outer coastal DEDK	OC DEDK	1,6	1,99	20%	3,04	2,58	15%
Coastal	II	Southern North Sea	SNS	3,8	3,33		2,54	2,31	9%
Shelf	III, IV	Atlantic Seasonally Stratified	ASS	1,8	0,64		2,21	2,14	3%
Shelf	II	Channel coastal shelf tidal	CCTI	2,3	1,62		2,28	2,16	5%
Shelf	II, III	Channel well mixed	CWM	1,3	0,88		2,20	2,17	1%
Shelf	II	Channel well mixed tidal influenced	CWMTI	1,5	0,78		2,08	2,02	3%
Shelf	II	Dogger Bank	DB	1,3	0,91		1,92	1,91	0%
Shelf	II	Eastern North Sea	ENS	1,2	1,06		1,96	1,80	8%
Shelf	IV	Gulf of Biscay coastal waters	GBCW	2,7	1,66		2,10	2,00	5%
Shelf	IV	Gulf of Biscay shelf waters	GBSW	2,0	0,82		1,35	1,31	3%
Shelf	II, III	Intermittently Stratified 1	IS1	1,8	1,16		2,53	2,52	0%
Shelf	II	Intermittently Stratified 2	IS2	1,7	1,42		2,50	2,49	0%
Shelf	II	Northern North Sea	NNS	1,1	0,70		1,87	1,85	1%
Shelf	II	Norwegian Trench	NT	1,7	1,19		2,64	2,42	8%
Shelf	II	Skagerak	SK	1,7	1,58		2,69	2,25	16%
Shelf	II, III	Scottish Sea	SS	1,5	1,30		2,28	2,26	1%

5.2 Comparison with earlier scenario results

Comparing model results for the current state between this study and the earlier model results reported by van Leeuwen et al. (2023), showed that the use of river loads consistent with OSPAR-RID data as input for the ecological model had a large impact on the model results (Figure 5-4, Figure 5-5). In Dutch assessment areas both winter mean DIN and DIP concentration in the new model results for the current state were much lower than in the previous simulations. Since the river loads in historic state scenarios are defined as a percentage nutrient load reduction compared to the current state, the nutrient concentrations in the scenario HS2+50% of the new model results can be lower than the HS2 scenario of the previous (Lenhart *et al* 2022) model study. This occurs for example in the Dutch assessment areas SNS, ENS and DB. In the ENS area the new estimate of nutrient conditions in the current state was similar to the estimate of pre-eutrophic reference conditions from the earlier model study.

This inconsistency is a problem when we try to use the models for estimating required nutrient reductions to meet the thresholds. These thresholds are based on the previous set of model simulations, based on ICG-EMO data. In Dutch coastal waters, thresholds would have been lower than current thresholds (based on ICG-EMO loads) if the river loads in the previous model runs (Lenhart *et al.* 2022, van Leeuwen *et al.* 2023) would have been consistent with OSPAR-RID data (as nutrient loads in the RID data are lower than in the ICG-EMO loads, see Figure 2.3). In other areas, for example in France, the thresholds would have been higher (as RID data are higher than ICG-EMO loads, see Figure 2.3). Without further analysis, there is no simple answer to the question which of the two river load datasets is more accurate.

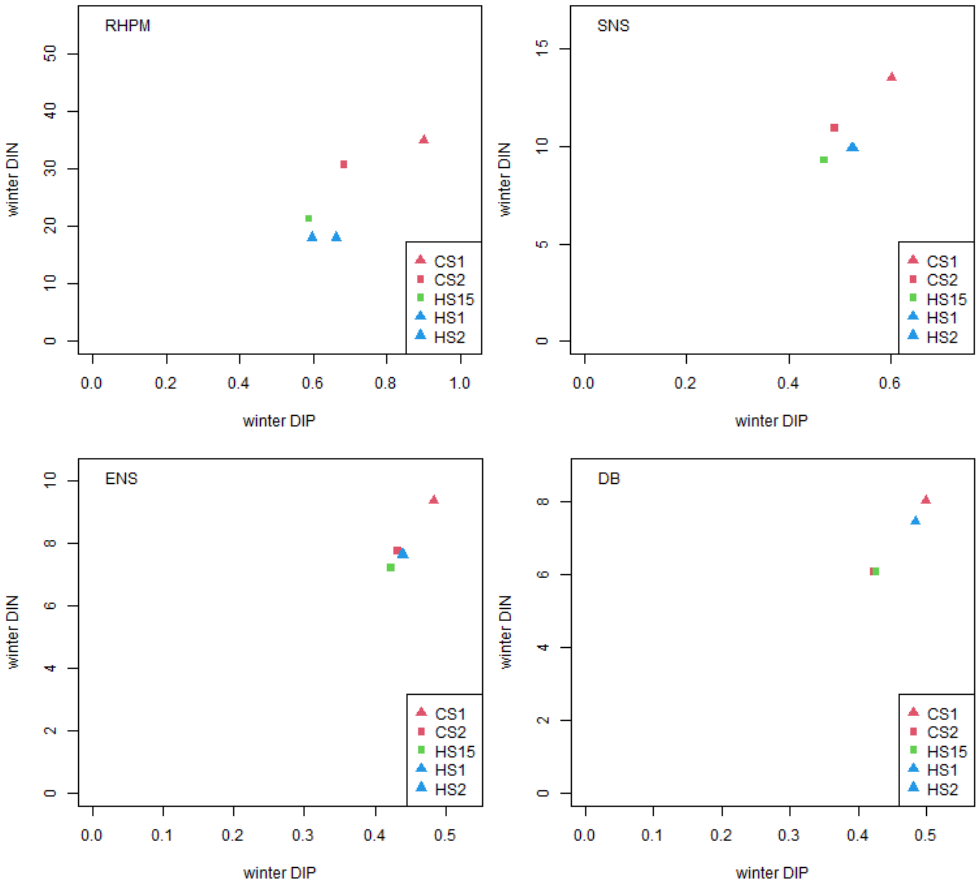

Figure 5-4 Winter nutrient concentrations in old (CS1, HS1, HS2) and new scenario simulations (CS2, HS15) in Dutch assessment areas: Rhine plume, southern North Sea, eastern North Sea and Dogger Bank.

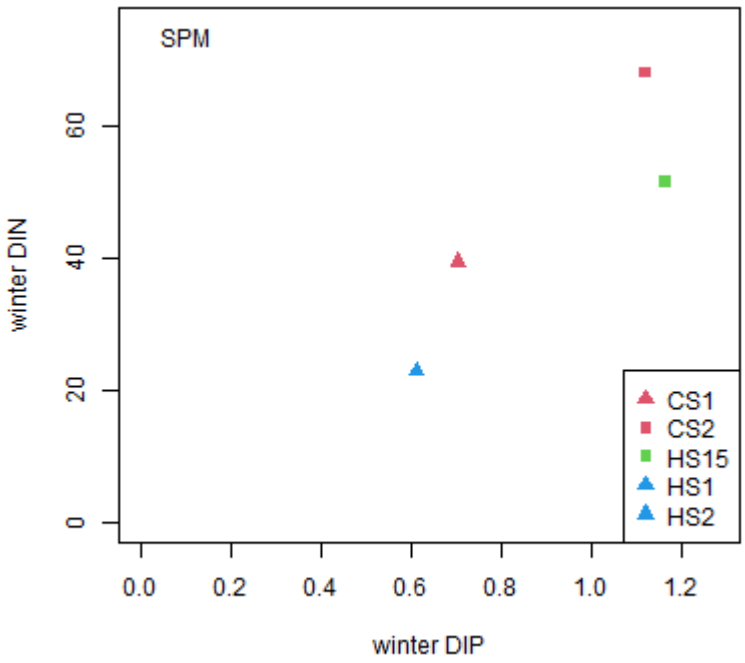

Figure 5-5 Winter nutrient concentrations in old (CS1, HS1, HS2) and new (CS2, HS15) scenario simulations for the Seine plume area.

5.3 Conclusions

Unsurprisingly, the reduced nutrient loads in the HS2+50% scenario resulted in lower nutrient and chlorophyll concentrations compared to the current state scenario, mainly in the river plumes and coastal areas.

The reduction in concentrations that was predicted by the model results seemed to be sufficient in most cases to achieve non-eutrophication status in the assessment areas that were assessed as being eutrophic in the COMP4 assessment.

In many coastal areas, a large difference exists in the modelled nutrient concentrations between the model simulations based on ICG-EMO data and those based on rescaled ICG-EMO data to match RID data. The difference is of similar magnitude as the difference between the current state scenario and the historic scenarios. This leads to an inconsistency between the model runs used to define the thresholds and the model runs used to estimate the maximum allowable inputs (MAI).

6 Changes in chlorophyll concentrations in response to reduced nutrient loads – *in situ* observations

6.1 Time series of *in situ* data

As a first approach for trend detection in the MWTL data we plotted all surface layer observations that passed the quality control and plotted them as time series. We fitted a trend line through the data with linear regression against time in R. Figure 6-1 shows an example of these time series and the fitted trend line at location Terschelling 10 km. We calculated the relative decrease in concentrations as the percentage change in concentrations from the beginning (1976) to the end (2021) of the fitted trend line (Table 6.1).

For dissolved inorganic nitrogen (DIN) all locations up to 70 km offshore showed a significant decreasing trend over the period 1976 to 2021. For dissolved inorganic phosphate (DIP) all locations up to 20 km offshore showed a significant decreasing trend and Terschelling 100 showed a weakly significant increasing trend. The decreasing trend in nitrogen loads in the nearby rivers, Rhine and Meuse, is much larger for DIP than for DIN (Rozemeijer *et al.* 2021). A potential reason why the decreasing trend in coastal waters is less strong for DIP than for DIN is, that for DIP some exceptionally high observations occurred in many time series (see for example Figure 6-1). These values had passed quality control but still seemed to be outliers. These observations obscure the detection of significant trends through linear regression of time series with all available observations.

The only locations with significant decreasing trends for both nutrients and for chlorophyll-a, were: Noordwijk 20 km and Terschelling 10 km. At the other locations no significant decrease in chlorophyll-a could be detected, despite 30-70% decreases in DIN concentrations and 50-100% decreasing trend in DIP. A 100% decrease in DIP concentrations means that the fitted trend line estimates DIP concentrations in 2021 to be close to zero. Obviously, this was an artefact of the linear regression of a trend that, in reality, was not linear. There was a particularly sharp drop in riverine P loads in the early 1990s due to the replacement of phosphates in detergents and improved wastewater treatment (Rozemeijer *et al.* 2021).

The results of this approach showed that there were strong decreasing trends in DIN and DIP concentrations in Dutch coastal waters in recent decades. But the outliers in the DIP time series and the strong variability of chlorophyll-a time series (which is under-sampled with the bi-weekly to monthly sampling data) obscured the accurate detection of trends with this simple linear regression approach.

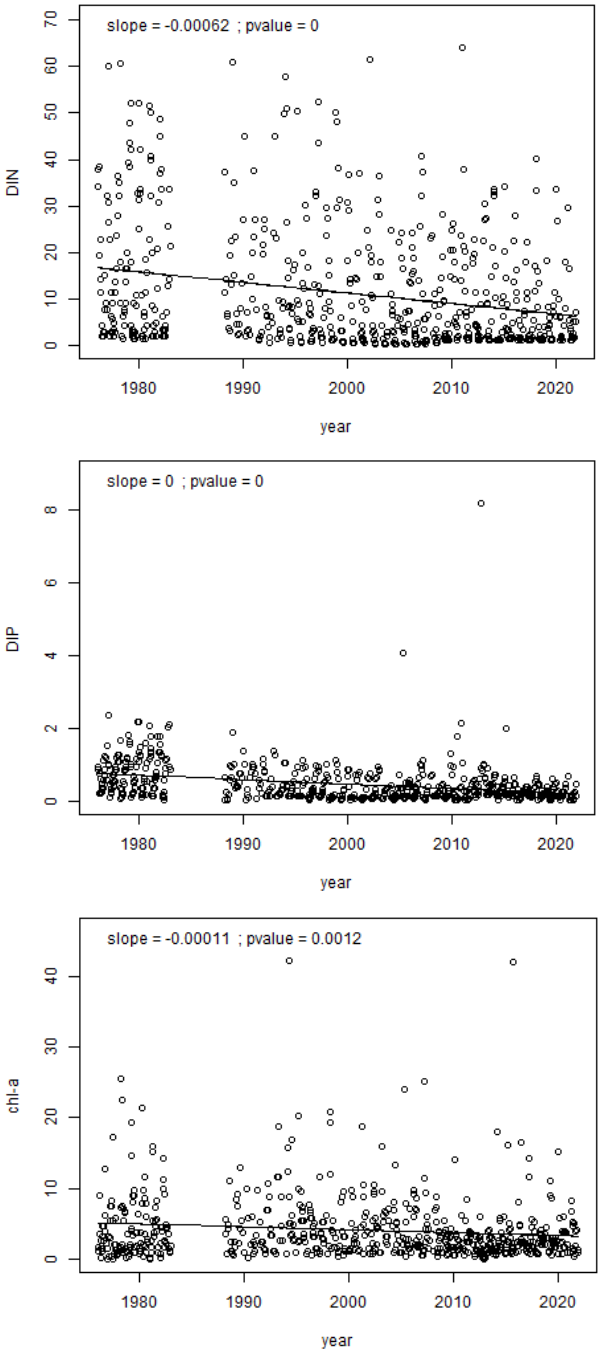

Figure 6-1 Example of trend detection by linear regression of non-aggregated time series data against time for DIN, DIP and chlorophyll-a at location Terschelling 10 km from the coast.

*Table 6.1 Percentage change in concentrations and statistical significance of decreasing trends in DIN, DIP and chlorophyll-a based on linear regression against time of non-aggregated time series (***p-value<0.001, **p-value<0.01, *p-value<0.05). Empty cells indicate no significant change.*

Location code	% decrease In DIN	% decrease in DIP	% decrease in chlorophyll-a
NOORDWK2	66 ***	100 ***	
NOORDWK10	69 ***	100 ***	
NOORDWK20	65 ***	93 ***	30 *
NOORDWK70	46 ***		
WALCRN2	44 ***	51 ***	
WALCRN20	58 ***	72 ***	
WALCRN70	33 **		
TERSLG10	61 ***	73 ***	36 **
TERSLG100		-43 *	
TERSLG135			70 *
TERSLG175			
TERSLG235			

6.2 MWTL data aggregated per decadal period

To reduce the impact of outliers and random noise due to temporal undersampling we applied an alternative approach for trend detection. We calculated median winter concentrations of DIN and DIP and growing season mean chlorophyll-a concentrations per decadal period. By taking the median value of winter DIP concentrations the impact of the outliers was much reduced. By integrating over multiple years, the seasonal mean and median concentrations were less affected by temporal undersampling.

Table 6.2 shows the percentual changes in DIN, DIP and chlorophyll-a concentrations between the 1980s and recent years. The significance of the change was based on a two-tailed t-test. Only 4 locations showed a significant decrease in DIN and/or DIP concentrations together with a significant decrease in growing season mean chlorophyll-a concentrations. Strikingly, the change in DIN and DIP concentrations was similar for both Walcheren 20 km (W20) and Terschelling 10 km (T10), but the response in chlorophyll-a concentrations was very different. At T10 the decrease in nutrients led to a 40% reduction in chlorophyll-a concentrations, while at W20 no significant reduction in chlorophyll-a concentrations was observed. At Noordwijk 70 km there was a significant decrease in chlorophyll-a concentrations, while there was no significant decrease in nutrient concentrations.
Figure 6-2 shows the median DIN and DIP concentrations for the different decadal periods. Comparing the concentrations in the 1980s (black circles: before the sharp drop in DIP concentrations in the early 1990s) and recent concentrations (blue circles) a major decrease in DIP concentrations was visible for the coastal locations (closer than 70 km from shore). DIN concentrations also showed a clear, though smaller, decrease. The locations Walcheren 20 km (W20) and Terschelling 10 km (T10) had very similar nutrient concentrations, both in the 1980s and in recent years. All locations closer than 70 km offshore had DIN/DIP ratios above 16 in winter, pointing at a tendency towards P-limitation. In the locations further offshore DIN/DIP ratios were close to or below 16, suggesting a higher probability of N-limitation.

*Table 6.2 Percentual change and statistical significance of decreasing trends in DIN, DIP and chlorophyll-a based a two-sided t-test between concentrations in the 1980s and recent years (***p-value<0.001, **p-value<0.01, *p-value<0.05). Grey numbers represent non-significant trends.*

Location code	% decrease in DIN	% decrease in DIP	% decrease in chlorophyll-a
NOORDWK2	19 **	66 ***	26 *
NOORDWK10	27 **	61 ***	29 **
NOORDWK20	22 *	57 ***	35 **
NOORDWK70	11	15	35 **
WALCRN2	17 ***	43 ***	7
WALCRN20	29 ***	54 ***	3
WALCRN70	2	8	27
TERSLG10	32 **	59 ***	41 ***
TERSLG100	20	4	-6
TERSLG135	18	9	-14
TERSLG175	-42	-35	-14
TERSLG235	1	-97 **	-34

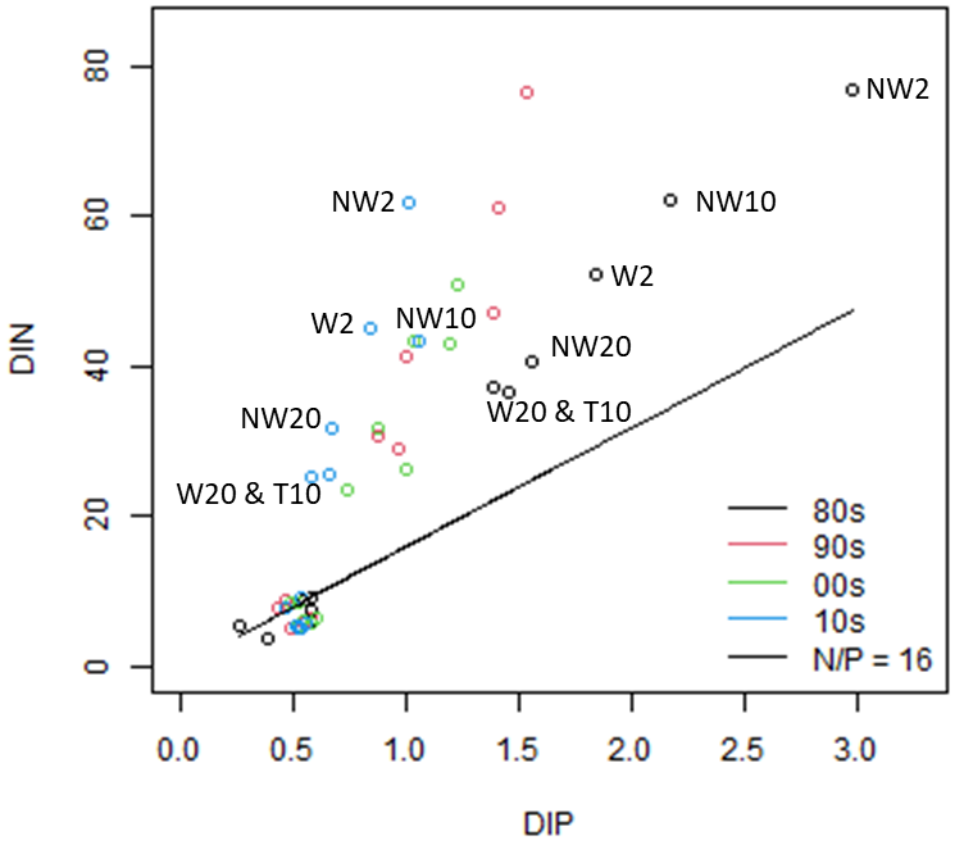

Figure 6-2 Medians of DIN and DIP concentrations in the four decadal periods

Figure 6-3 shows the same data points as Figure 6-2 above, with the colours of the circles representing the growing season mean chlorophyll-a concentrations per decade. The chlorophyll-a concentrations clearly decreased with decreasing DIN and DIP concentrations (towards the origin). If phytoplankton growth is limited by phosphorus availability only, one would expect to see the gradient in colours mainly in vertical bands. If phytoplankton growth is limited only by nitrogen, one would expect to see the gradient mainly in horizontal bands. Figure 6-3 does not show clear vertical or horizontal bands. For the offshore station the pattern looks mostly like horizontal bands, indicating nitrogen limitation.

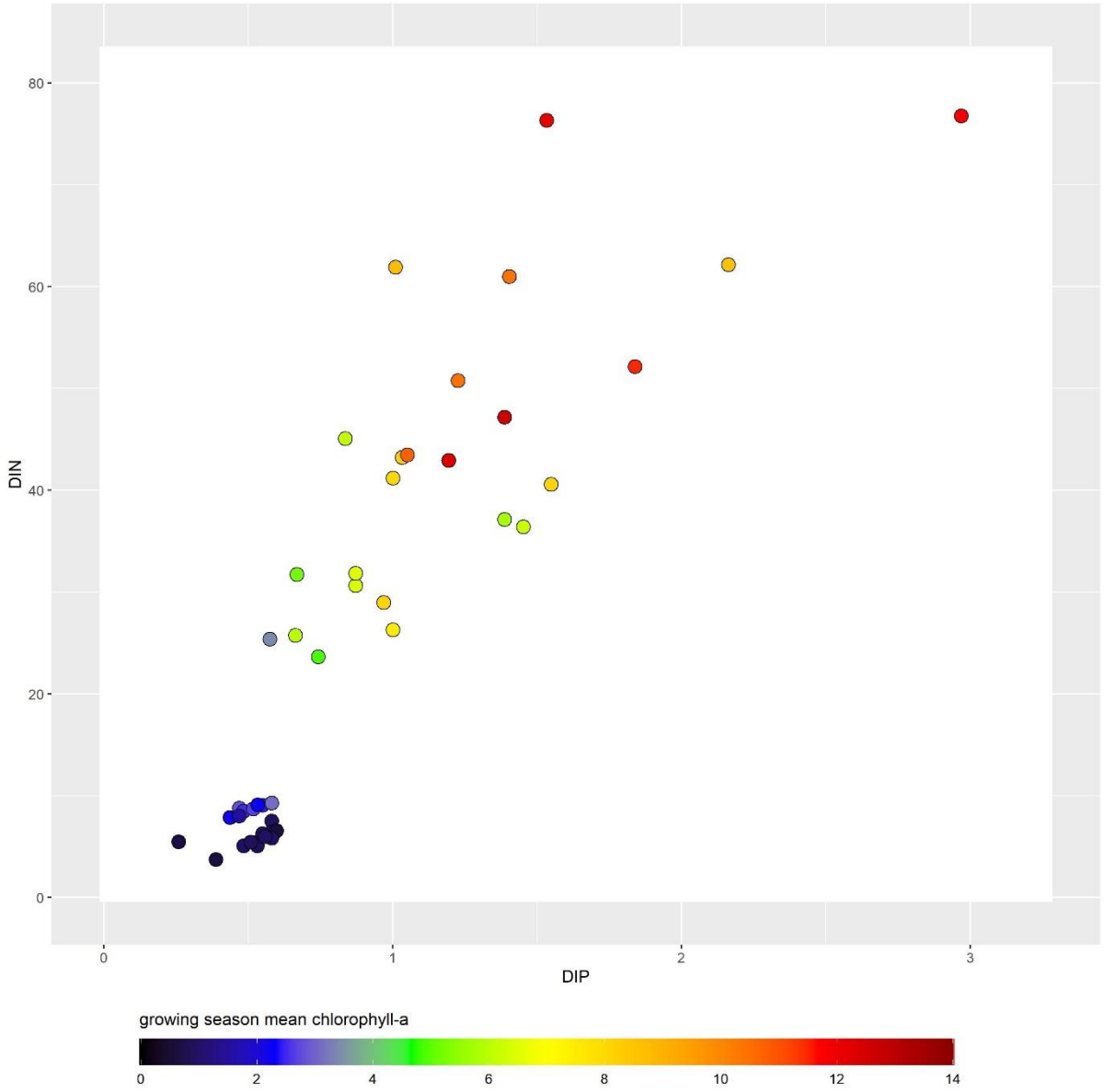

Figure 6-3 Observed growing season mean chlorophyll concentrations (expressed by the colour scale) as a function of winter DIN and winter DIP concentrations.

6.3 Response curve of chlorophyll to DIN and DIP in *in situ* data

The main question for this data analysis was, whether growing season mean chlorophyll-a concentration decreased linearly and proportionally to decreasing availability of nutrients, approximated by their (median) winter concentrations. If the nutrient content of phytoplankton

cells remains constant one would expect to see a decrease in chlorophyll-a concentrations that is proportional to the decrease of the limiting nutrient.
Figure 6-4 shows the observed growing season mean chlorophyll-a concentrations as a function of median winter DIN and DIP concentrations for the locations with significant trends in nutrient concentrations and chlorophyll-a concentrations (Table 6.2). Chlorophyll-a concentrations showed approximately a linear increase with both DIN and DIP concentrations. For DIP the slope of the relation deviated between the 1980s and the other decades. This suggested that phytoplankton growth was limited by nitrogen in the 1980s, leading to lower chlorophyll-a concentrations than would be expected based on the slope of the relation between DIP and chlorophyll-a in later decades.

Figure 6-5 shows the relative decrease in chlorophyll-a concentration against the relative decrease in nutrient concentrations, between the 1980s and recent years to compare with Figure 2-6 in §2.6. This shows that the decrease in chlorophyll-a concentrations between the 1980s and recent years was approximately proportional to the decrease in DIN concentrations (25% reduction in DIN and 30% reduction in DIP). The reduction in chlorophyll-a concentrations (30%) was approximately half of the reduction in DIP concentrations (60%).

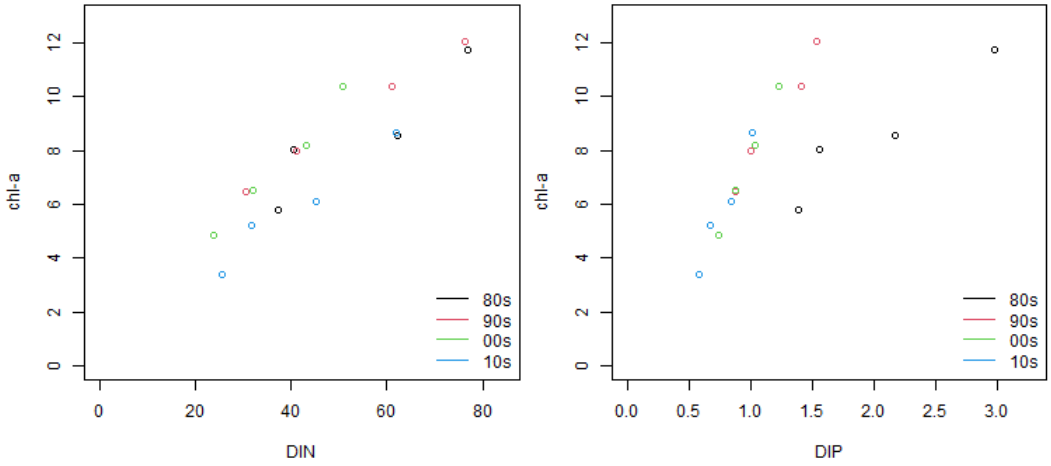

Figure 6-4 Decadal growing season mean chlorophyll-a concentrations as a function of winter median DIN (left) and DIP (right) concentrations for 4 different decades for 4 locations with significant trends.

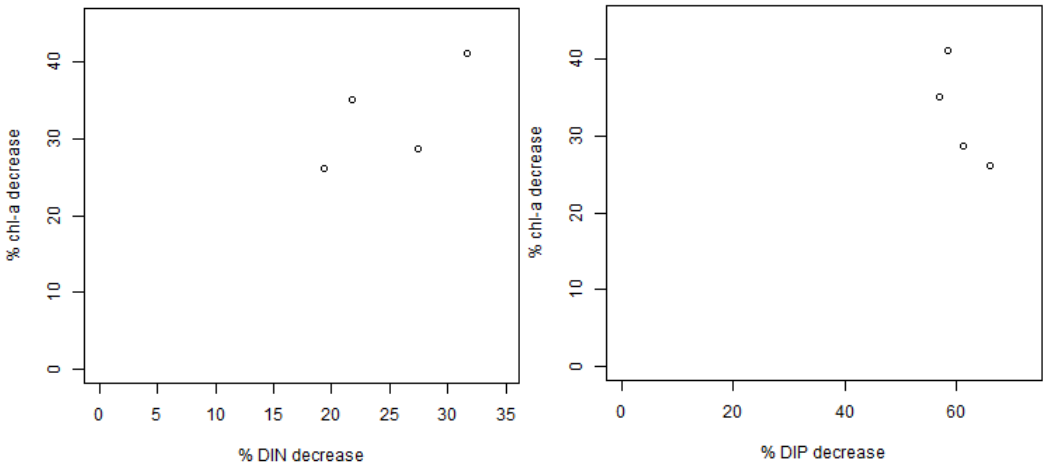

Figure 6-5 Relative decreases (%) in growing season mean chlorophyll-a concentrations as a function of relative decreases (%) in winter median DIN (left) and DIP (right) concentrations between the 80s and recent years (10s) at 4 locations with significant trends.

As the relation between DIP and chlorophyll-a concentrations differed between the 1980s and later decades we checked if the response of chlorophyll to decreasing DIP concentrations was proportional in the years after the sharp drop in phosphate loads from rivers. Figure 6-6 compares the decreases in nutrient concentrations and chlorophyll-a concentrations between the 1990s and recent years. This showed that, after the 1980s, the decrease in chlorophyll-a concentrations was proportional to the decrease in DIP concentrations (~40%). The decrease in DIN concentrations over this period was smaller than the decrease in chlorophyll-a concentrations, which was another indication that phytoplankton growth was not limited by nitrogen in these decades.

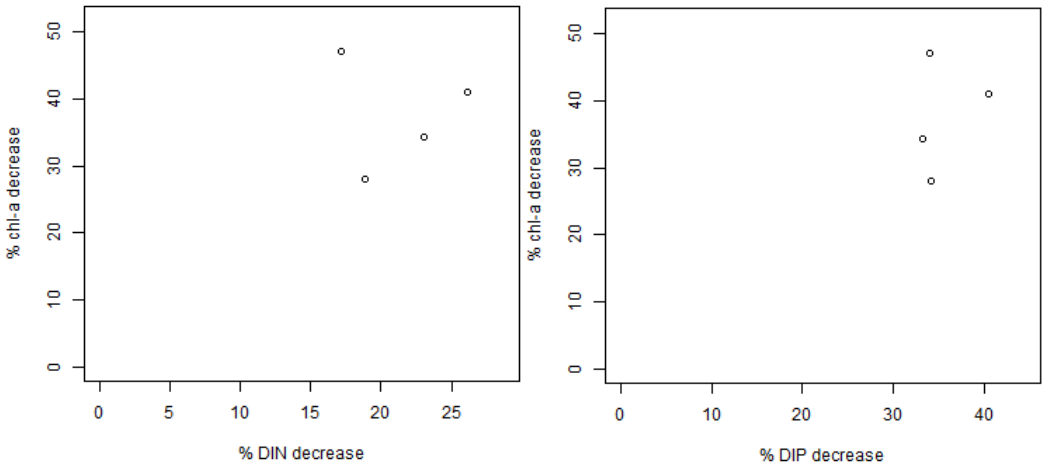

Figure 6-6 Relative decreases (%) in growing season mean chlorophyll-a concentrations as a function of relative decreases (%) in winter median DIN (left) and DIP (right) concentrations between the 1990s and recent years (2010s) at the four locations with significant trends.

6.4 Comparison with response curve in model

The comparison of model responses by van Leeuwen et al (2023), shown in Figure 2.6 of this report showed that the Deltares model shows a rather linear and proportional response of chlorophyll-a concentrations to nutrient reduction: both for N and P reduction. The data analysis above shows that this is a realistic response for P reduction in nearshore Dutch coastal waters since the early 1990s. In this period and area P appears to be the limiting nutrient controlling growing season mean chlorophyll-a concentrations. In Dutch offshore waters N appears to be the limiting nutrient. However, due to the strong dilution of river water inputs with oceanic waters in these areas, no significant decreasing trend in nitrogen is observed and we cannot test whether the response in chlorophyll-a concentrations would be linear and proportional to the reduction in nitrogen concentrations.

Figure 6-7 compares the relation between winter median DIN and DIP and growing season mean chlorophyll-a in MWTL-data (same as Figure 6.3) and the same relation in model results. The model results are shown as area means of Dutch assessment areas for the current state scenario and HS2+50% 1.5 scenario from this model study. The model results cover only a small part of the range of DIN and DIP concentrations that are covered by the observations, so we cannot conclude from this comparison whether the model response corresponds with patterns in observation data. However, within the range of the model results the pattern is similar to the pattern in the observations, although simulated chlorophyll-a concentrations are slightly too high, which is also shown in chapter 4.

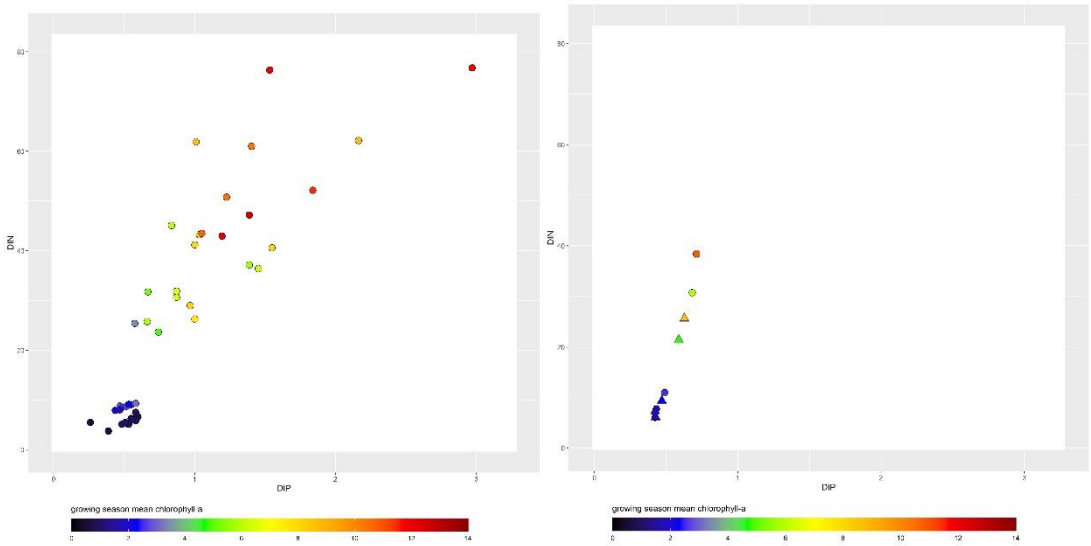

Figure 6-7 Observed (left) and modelled (right) chlorophyll concentrations (in µg/l) (see colour scale) plotted against modelled DIN and DIP concentrations (in µM). The observations (left) represent period medians and means per observation location. The model results represent area means for Dutch assessment areas from the current state scenario (circles) and historic scenario + 50% (triangles).

6.5 Conclusions

Since the sharp drop in riverine phosphate loads in the early 1990s, decreases in chlorophyll-a concentrations in most locations in Dutch coastal waters have been proportional to decreases in winter median DIP concentrations. However, in coastal waters along the Walcheren transect, close to the Belgian border, chlorophyll-a concentrations have not significantly decreased over the same period. This was in contrast to location Terschelling 10 km offshore, that had similar nutrient concentrations and showed decreases in chlorophyll concentrations. Possibly, the relatively turbid waters in coastal waters near Walcheren explain the different DIP-chlorophyll-a relations at this site compared to other areas in Dutch coastal waters. This requires further investigation.

7 Discussion

In this report, we have quantified transboundary nutrient transport in the NE Atlantic. This was done by carrying out tracer studies with riverine nutrient loads that were aligned with the RID data. The results (Chapter 3) provide estimates of the contributions of rivers, atmospheric deposition, outflow from the Baltic Sea and input from the Atlantic Ocean to the nutrient concentrations in each of the assessment areas that are used by OSPAR in the eutrophication assessment. Those results are a basis for further work to establish Maximum Allowable Inputs of nutrients.
We explored the response in chlorophyll concentrations to changes in nutrient loads by running a model simulation with reduced riverine loads, supplementing earlier modelling work by ICG-EMO (Chapter 5). In addition, we used *in situ* data from the Dutch part of the Noth Sea over a 40-year period to analyse the effects of changes in riverine loads of total-P and total-N on the concentrations of chlorophyll (Chapter 6).

7.1 Impact of river input data

In this study we derived correction factors to make the model river loads (taken from the ICG-EMO database) consistent with the loads in the RID database. This improved the estimates of total riverine nutrient loads to the model domain in areas where the ICG-EMO database is less complete. This was the case, for example, for the loads from Spain, France, Denmark and Norway. However, the RID database does not include the geographical position of individual loads. For the application in the model, we solved this by splitting up the RID loads over the river mouths available in the ICG-EMO database. That may have led to errors in the spatial patterns of nutrient concentrations, with an overestimation directly downstream of river mouths that were in the ICG-EMO database and an underestimation at other locations that were not in the ICG-EMO database (but actually do receive anthropogenic loads).
The question of how to improve the spatial distribution of RID loads in OSPAR ecosystem models at locations that are currently not included in ICG-EMO has to be addressed by ICG-EMO in the ongoing update of the river database that is aimed at making it more consistent with the RID data.
The alignment of the riverine loads from the ICG-EMO database with the RID data, also resulted in substantial changes in river loads in some cases, as shown in Annex B. Clearly, the uncertainty in the river load estimates has a strong impact on the model results and the confidence in those results, in particular in those areas where the difference between the ICG-EMO river loads and the RID data is large.
The current OSPAR thresholds were based on estimates of pre-eutrophic loads derived from ICG-EMO data and estimates of pre-eutrophic conditions. Maximum allowable inputs will be based on the RID-compliant river load dataset, which may give rise to inconsistencies between the current thresholds and MAIs. This stresses the need to come to an agreement between Contracting Parties on the river loads that will be used as the basis for further decision making. This topic is not in the scope of the study reported here but needs an urgent solution for the follow-up of the ICG-EMO work.

7.2 Model validation

Changes in the model setup have led to improvements in results. The biggest change was the introduction of dissolved organic fractions of carbon, nitrogen and phosphorus in the model. This led to slower re-mineralization of nutrients in the model and improved the model's performance to capture chlorophyll-a concentrations. Growing season concentrations were less overestimated than in previously reported OSPAR simulations using Delft3D FM.

Concentrations were, however, still overestimated in more offshore areas. The reason for this needs to be investigated in future studies.

We also compared model outputs against the OSPAR satellite product. This provided data at higher temporal and spatial resolution for the model. Time-series comparisons for example, allowed us to better assess chlorophyll-a concentration variations during the growing season, while the lower frequency of MWTL measurements does not always capture chlorophyll peaks or the precise timing of the bloom offset or the phytoplankton decline at the end of the growing season. This first comparison of our model to satellite data clearly showed the usefulness of including satellite data in future model validations.

7.3 Transboundary nutrient transport

The results presented in this report provided an estimate of the contribution of the various anthropogenic sources (riverine and atmospheric deposition) to the nutrient concentrations in the assessment areas used by OSPAR. Due to this new spatial division in the OSPAR COMP4 assessment areas, a direct comparison with the results from previous studies was not straightforward. In our current study, only conservative transport (i.e., excluding biogeochemical/ecological processes) was applied. Earlier model applications have shown that estimates of the relative contribution of sources based on conservative transport show only minor deviations from the results based on an ecological model including those processes (Blauw *et al.* 2006).

There have been various studies quantifying transboundary nutrient transport in the NE Atlantic, with the main focus on the Greater North Sea. Earlier Deltares models have been used in the past for tracer studies in the Channel and southern North Sea, for the period 1997-2003 (Blauw *et al.* 2006, Los *et al.* 2014, see their Figure 5). Other studies using the MIRO&CO model for the Channel and Southern Bight of the North Sea looked at the period 1991-2003 (Lacroix *et al.* 2007) and the period 2000-2010 (Dulière *et al.* 2017, see their Figure 11). It should be noted that there are differences between the various model applications, in transport patterns, spatial resolution and riverine loads that were used. However, the overall spatial picture from all studies shows a similar pattern. Summarizing, for the Greater North Sea, the influence of nutrient loads from river sources on the French Channel coast is dominant in the Channel area (in combination with a large influence from the Atlantic Ocean) and extends into the more offshore waters of the southern North Sea, up to the assessment areas Dogger Bank and Eastern North Sea. The main river sources on the English east coast are Humber and Thames, and the plumes of these rivers extend along the English coast (assessment areas Humber plume and Thames plume) and into the assessment areas southern North Sea, Dogger Bank and Eastern North Sea. River sources from Belgium and the Dutch North Sea coast (Scheldt, Meuse and in particular Rhine) have the largest impact in the assessment areas Scheldt, Meuse and Rhine plume, but also contribute to the assessment areas southern North Sea, Ems and Elbe plume, Outer Coastal DEDK and German Bight Central. The Elbe plume assessment area shows influence from a mixture of rivers, is dominated by loads from the river Elbe but with significant contributions from the other large rivers along the SE coast of the North Sea.
Compared to the earlier published studies and the applications of earlier Deltares models (using ICG-EMO river data), the results from our current model application (Chapter 3) showed a much higher contribution from the river sources along the French Channel coast, that extended into the southern North Sea and along the Dutch and German coast. The main reason for this much higher estimate in our model results may have been the much higher riverine loads from the French Channel coast (as a consequence of the alignment of the ICG-EMO data with the RID data; see Annex B).
In the EMOSEM project two marine ecosystem models (ECO-MARS3D, MIRO&CO) were used to quantify the contribution of various sources to winter phosphate and nitrate

concentrations in the Bay of Biscay, the English Channel and the southern North Sea for the period 2000-2010 (Ménesguen et al. 2018, see their Figure 6). Again, those results show that the influence of river discharges on the French Channel coast extends into the Southern Bight of the North Sea (i.e. affecting the assessment area Southern North Sea), but the relative contributions of inputs from the rivers Scheldt, Meuse and Rhine are much larger along the Dutch coast, in comparison to our model results.
Painting *et al.* (2013) (see their Figure 4) showed results from the application of the GETM-ERSEM-BFM model run by Cefas for the Greater North Sea in 2002. Lenhart & Große (2018) (see their Figure 4) did a tracer study for total nitrogen in the greater North Sea for 2006-2014.
Atmospheric deposition of nitrogen is a significant source in many parts of the Greater North Sea (this study, Troost *et al.* 2013).

7.4 Chlorophyll response to nutrient reduction

The analysis of *in* situ data clearly showed that lower chlorophyll concentrations were positively correlated with winter nutrient concentrations. Due to the strong correlation between winter DIN and winter DIP concentrations, the effect of changes in winter DIN concentrations cannot be analysed separately from the effect of changes in winter DIP concentrations. The analysis did not take into account the effect of any trends in underwater light climate. The difference in nutrient-chlorophyll relations between the 1980s and later years suggested that P-limitation of phytoplankton growth became more important in the years after 1990, in Dutch coastal waters. Loebl *et al.* (2009) also found potential limitation of phytoplankton by phosphate and silicate in Dutch coastal waters, based on analysis of *in situ* inorganic nutrient concentrations. However, they also noted that DIN concentrations are a good predictor of the spatial patterns in phytoplankton biomass. The role of organic nutrients and the fast remineralisation of phosphorus may lower the actual P-limitation. Increasing importance of P-limitation in Belgian coastal waters was inferred from changes in riverine nutrient loads (Passy *et al.* 2013). Based on results from bio-assays, Burson *et al.* (2016) also concluded that there is a gradient from co-limitation of phosphate and silicate in the coastal waters, particularly in spring, to nitrogen limitation in offshore waters.

Similar to the in situ data, the model results also indicated that there was a clear response of chlorophyll to changes in nutrient loads, in particular in the assessment areas with significant freshwater influence.

8 Recommendations

- For the understanding of the effects of nutrient enrichment on the marine environment, reliable information on the nutrient sources is essential. The currently available RID data provide estimates but lack the more detailed spatial and temporal information on riverine sources that is necessary for the use in ecosystem models. The ICG-EMO database on riverine sources has more detailed information, but differences between both databases result in uncertainty in the estimates of riverine loads. This uncertainty needs to be resolved in order to provide a reliable and accurate basis for decisions on maximum allowable loads.
- It should also be noted that the COMP4 thresholds (OSPAR 2022) were based on the current data in the ICG-EMO riverine loads database and need to be evaluated if the riverine loads are changed.
- Atmospheric deposition is a significant source of nitrogen in many parts of the NE Atlantic. It is recommended to take this into account in the analysis. Analyses looking at nutrient-chlorophyll relations could be biased if only riverine loads are considered. If the analysis looks at the relations between concentrations of nutrients and chlorophyll, the effects of atmospheric deposition are included.
- To increase our understanding of the dose-response relation between N, P and chlorophyll, the model results from the ICG-EMO ensemble modelling exercise need to be evaluated on the responsiveness of the models to changes in nutrient loads. That analysis should simultaneously be accompanied by an analysis of a larger dataset of *in situ* observations. For the latter analysis, building a dataset with a large spatial coverage to complement the results of the analysis presented in this report would be very valuable. Our current analysis has not yet considered the effect of light limitation, but obviously this should also be taken into account.

Satellite data on chlorophyll concentrations provide information at a much higher spatial and temporal resolution than the *in situ* data. The use of satellite data in the model validation can improve the evaluation of the model results and should be included, together with *in situ* data, in future work by ICG-EMO.

9 References

Axe, P., L. Sonesten, E. Skarbövik, W. Leujak and L. Nielsen (2023). Inputs of Nutrients to the OSPAR Maritime Area. *Quality Status Report 2023*. London, OSPAR Publication number 930/2022

Blauw, A.N., K.E. van de Wolfshaar and H. Meuwese (2006). Transboundary nutrients in the North Sea. Delft, WL|Delft Hydraulics, report Z4188.00, 75 pp.

Blauw, A.N., H.F.J. Los, M. Bokhorst and P.L.A. Erftemeijer (2008). GEM: a generic ecological model for estuaries and coastal waters. *Hydrobiologia* 618: 175-198.

Burson, A., M. Stomp, L. Akil, C.P.D. Brussaard and J. Huisman (2016). Unbalanced reduction of nutrient loads has created an offshore gradient from phosphorus to nitrogen limitation in the North Sea. *Limnology and Oceanography* 61: 869-888.

Dulière, V., N. Gypens, C. Lancelot, P. Luyten and G. Lacroix (2017). Origin of nitrogen in the English Channel and Southern Bight of the North Sea ecosystems. *Hydrobiologia*: 1-21.

HASEC (2023). Summary record of the meeting of the Hazardous Substances and Eutrophication Committee (HASEC). London, OSPAR, HASEC meeting, Edinburgh 20-24 March 2023 HASEC 22/11/1, 42 pp.

Lacroix, G., K. Ruddick, N. Gypens and C. Lancelot (2007). Modelling the relative impact of rivers (Scheldt/Rhine/Seine) and Western Channel waters on the nutrient and diatoms/*Phaeocystis* distributions in Belgian waters (Southern North Sea). *Continental Shelf Research* 27: 1422-1446.

Lenhart, H.-J., D.K. Mills, H. Baretta-Bekker, S.M. van Leeuwen, J.v. der Molen, J.W. Baretta, M. Blaas, X. Desmit, W. Kühn, G. Lacroix, H.J. Los, A. Ménesguen, R. Neves, R. Proctor, P. Ruardij, M.D. Skogen, A. Vanhoutte-Brunier, M.T. Villars and S.L. Wakelin (2010). Predicting the consequences of nutrient reduction on the eutrophication status of the North Sea. *Journal of Marine Systems* 81: 148-170.

Lenhart, H.-J. and F. Große (2018). Assessing the Effects of WFD Nutrient Reductions Within an OSPAR Frame Using Trans-boundary Nutrient Modeling. *Frontiers in Marine Science* 5.

Lenhart, H., A. Blauw, X. Desmit, L. Fernand, R. Friedland, B. Heyden, O. Kerimoglu, G. Lacroix, A. van der Linden, J. van der Molen, M. Plus, T. Prins, I. Ruvalcaba Baroni, T. Silva, C. Stegert, D. Thewes, T. Troost, L. Vilmin and S. van Leeuwen (2022). ICG-EMO report on model comparison for historical scenarios as basis to derive new threshold values. London, OSPAR, Publication Number: 895/2022, 66 pp.

Loebl, M., F. Colijn, J.E.E. van Beusekom, J.G. Baretta-Bekker, C. Lancelot, C.J.M. Philippart, V. Rousseau and K.H. Wiltshire (2009). Recent patterns in potential phytoplankton limitation along the Northwest European continental coast. *Journal of Sea Research* 61: 34-43.

Los, F.J., T.A. Troost and J.K.L. Van Beek (2014). Finding the optimal reduction to meet all targets—Applying Linear Programming with a nutrient tracer model of the North Sea. *Journal of Marine Systems* 131: 91-101.

Ménesguen, A., X. Desmit, V. Dulière, G. Lacroix, B. Thouvenin, V. Thieu and M. Dussauze (2018). How to avoid eutrophication in coastal seas? A new approach to derive river-specific combined nitrate and phosphate maximum concentrations. *Science of The Total Environment* 628–629: 400-414.

OSPAR (2022). The Common Procedure for the Identification of the Eutrophication Status of the OSPAR Maritime Area. OSPAR Agreement 2022-07 (Replaces Agreement 2013-08), 96 pp.

OSPAR (2023). Eutrophication Thematic Assessment. *Quality Status Report 2023,* London, OSPAR, Publication Number: 843/2022, 62 pp.

Painting, S., J. Foden, R. Forster, J. van der Molen, J. Aldridge, M. Best, P. Jonas, D. Hydes, P. Walsham, L. Webster, M. Gubbins, M. Heath and S. O'Boyle (2013). Impacts of

climate change on nutrient enrichment. *Marine Climate Change Impacts Science Review*: 219-235.

Passy, P., N. Gypens, G. Billen, J. Garnier, V. Thieu, V. Rousseau, J. Callens, J.Y. Parent and C. Lancelot (2013). A model reconstruction of riverine nutrient fluxes and eutrophication in the Belgian Coastal Zone since 1984. *Journal of Marine Systems* 128: 106-122.

Rozemeijer, J., R. Noordhuis, K. Ouwerkerk, M. Dionisio Pires, A. Blauw, A. Hooijboer and G.J. van Oldenborgh (2021). Climate variability effects on eutrophication of groundwater, lakes, rivers, and coastal waters in the Netherlands. *Science of The Total Environment* 771: 145366.

Seitzinger, S.P., J.A. Harrison, E. Dumont, A.H. Beusen and A. Bouwman (2005). Sources and delivery of carbon, nitrogen, and phosphorus to the coastal zone: An overview of Global Nutrient Export from Watersheds (NEWS) models and their application. *Global Biogeochemical Cycles* 19.

Troost, T.A., M. Blaas and F.J. Los (2013). The role of atmospheric deposition in the eutrophication of the North Sea: A model analysis. *Journal of Marine Systems* 125: 101-112.

Troost, T.A., A. de Kluijver and F.J. Los (2014). Evaluation of eutrophication variables and thresholds in the Dutch North Sea in a historical context — A model analysis. *Journal of Marine Systems* 134: 45-56.

van der Kaaij, T., T. van Kessel, T. Troost, P. Herman, L. van Duren and N. Villars (2017). Modelondersteuning MER winning suppletie- en ophoogzand Noordzee 2018 – 2027. Delft, Deltares, Rapport nr 1230888-002-ZKS-0006, 75 pp.

van Leeuwen, S.M., H.-J. Lenhart, T.C. Prins, A. Blauw, X. Desmit, L. Fernand, R. Friedland, O. Kerimoglu, G. Lacroix, A. van der Linden, A. Lefebvre, J. van der Molen, M. Plus, I. Ruvalcaba Baroni, T. Silva, C. Stegert, T.A. Troost and L. Vilmin (2023). Deriving pre-eutrophic conditions from an ensemble model approach for the North-West European seas. *Frontiers in Marine Science* 10:1129951.

Zijl, F., S. Laan, L. Leummens, T. Zijlker, T. van Kessel, V. van Zelst, L. Jaksic, L. Vilmin, L. Schneider and L. van Duren (2023a). Scenario studies on potential ecosystem effects in future offshore wind farms in the North Sea. Delft, Deltares, Report 11208071-001-ZKS-0010, 84 pp.

Zijl, F., T.D. Zijlker, S.C. Laan and J. Groenenboom (2023b). 3D DCSM-FM: a sixth-generation model for the NW European Shelf : 2022 release. Delft, Deltares, Report 11208054-004-ZKS-0003, 68 pp.

A Maps of the OSPAR assessment areas and Wadden Sea assessment areas

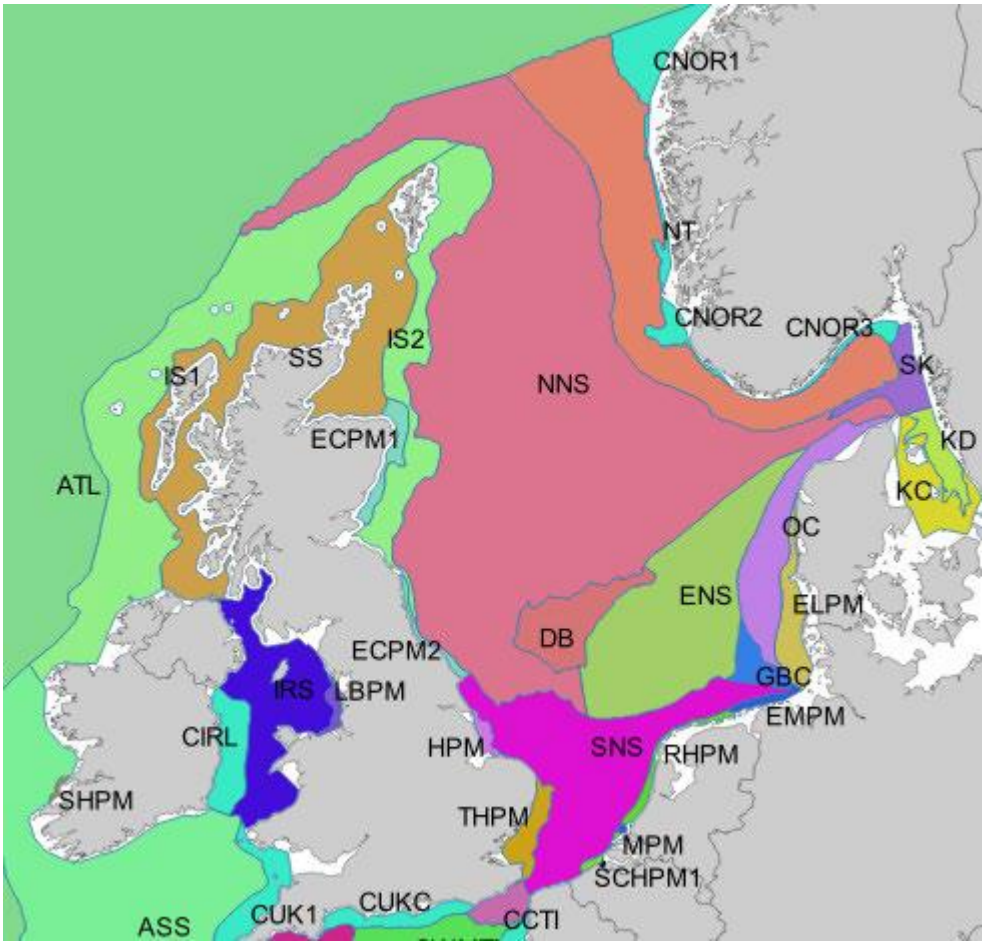

Figure A.1 Detailed view of the assessment areas in OSPAR region II and III (source: OSPAR, 2022)

.

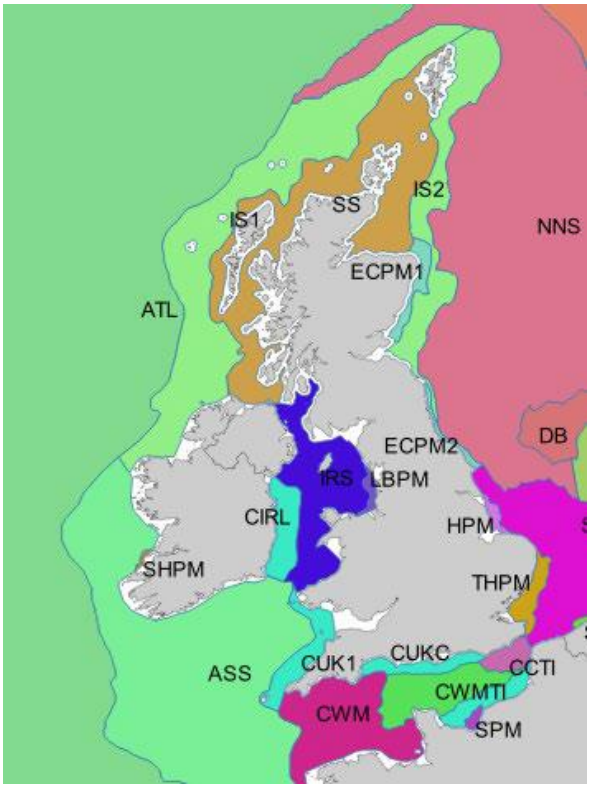

Figure A.2 Detailed view of the assessment areas in OSPAR region III (source: OSPAR, 2022).

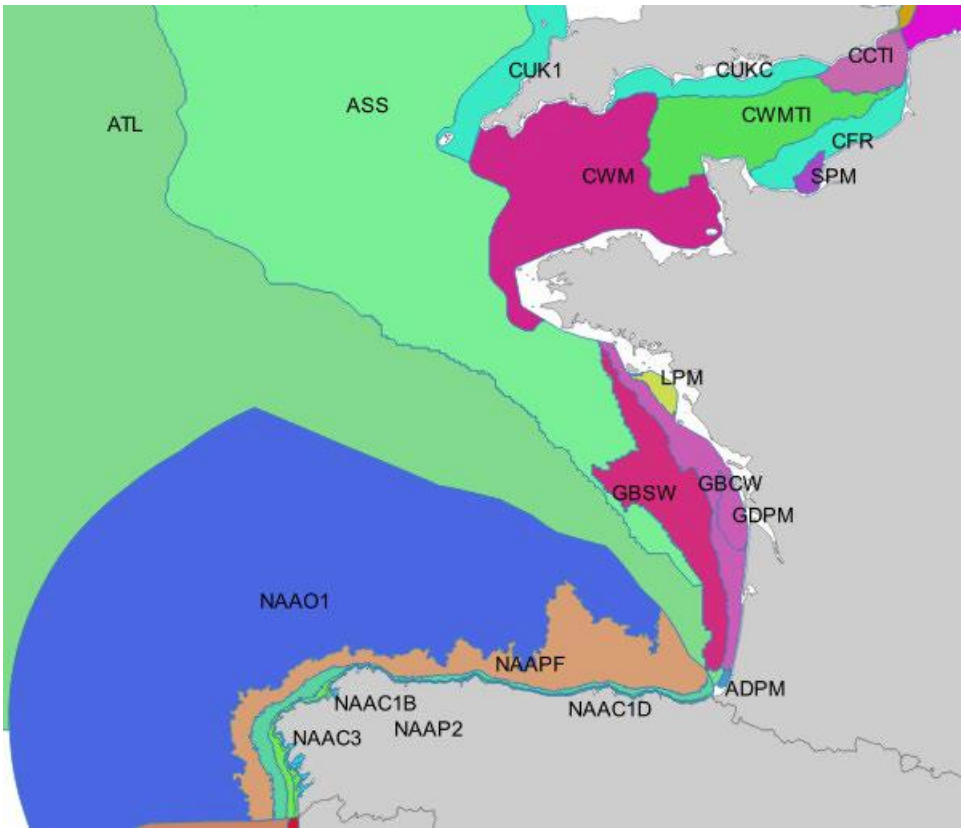

Figure A.3 Detailed view of the assessment areas in OSPAR region II and IV (source: OSPAR, 2022).

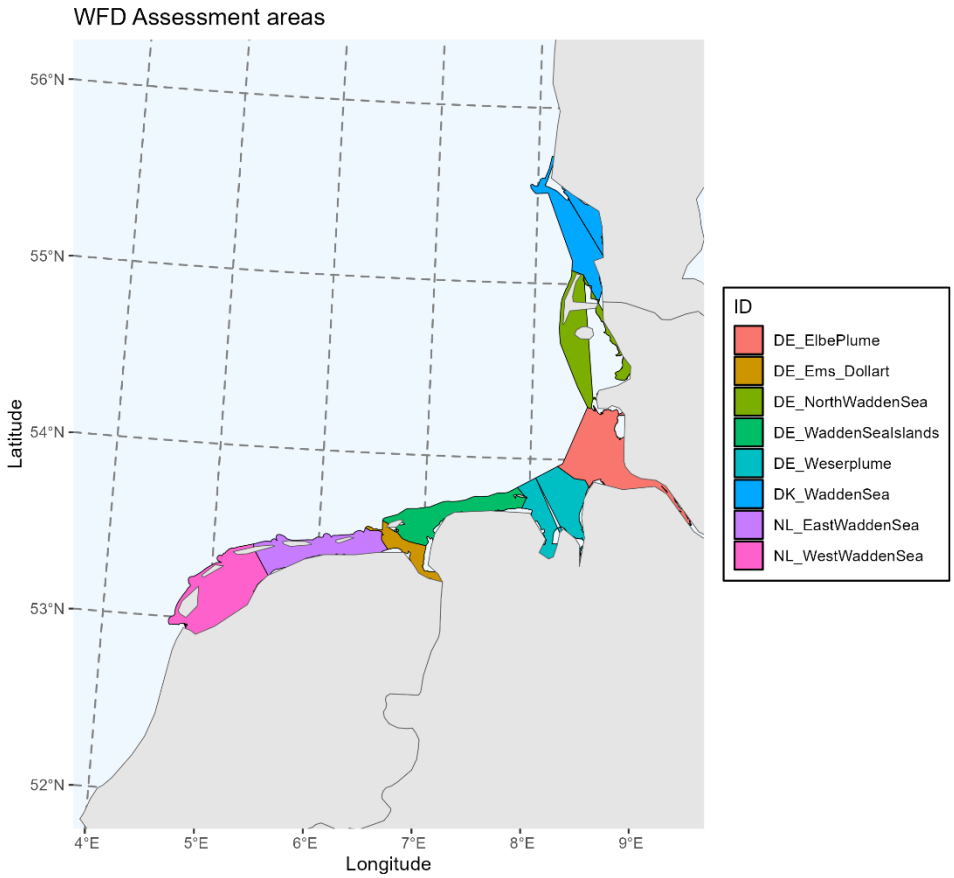

Figure A.4 Overview of WFD assessment areas in the Wadden Sea.

B Summary of nutrient loads per RID area and correction factors applied to ICG-EMO-derived model inputs

Table B.1 Summary of yearly total N and total P loads reported per RID area in kton/year, loads derived from ICG-EMO river data and factors applied to model inputs to be consistent with RID data.

RID area	Year	Total Nitrogen			Total Phosphorus		
		RID load	ICG-EMO load	Factor	RID load	ICG-EMO load	Factor
Atlantic (ES)	2012	39.4	10.6	3.70	3.98	0.18	22.61
	2013	14.0	10.4	1.35	1.52	0.18	8.65
	2014	61.2	9.7	6.31	2.51	0.17	14.39
	2015	27.6	11.1	2.48	2.61	0.18	14.57
	2016	28.9	11.2	2.57	2.47	0.18	13.70
	2017	16.4	11.2	1.47	1.16	0.18	6.44
Atlantic (FR)	2012	354.6	232.8	1.52	9.42	3.55	2.65
	2013	557.5	145.0	3.85	14.37	3.57	4.02
	2014	415.3	105.1	3.95	10.39	2.21	4.69
	2015	239.4	139.8	1.71	5.92	2.53	2.34
	2016	271.1	116.8	2.32	5.84	2.25	2.60
	2017	134.4	85.5	1.57	3.61	1.58	2.28
Atlantic (IE)	2012	18.6	9.3	1.99	0.79	0.30	2.60
	2013	16.0	8.4	1.90	0.71	0.29	2.42
	2014	21.3	8.1	2.64	0.81	0.26	3.08
	2015	23.6	9.0	2.62	0.88	0.40	2.19
	2016	15.1	8.4	1.81	0.61	0.29	2.12
	2017	18.9	9.4	2.02	0.74	0.34	2.18
Atlantic (UK)	2012	27.7	78.9	0.35	3.94	3.15	1.25
	2013	28.3	78.6	0.36	3.85	3.18	1.21
	2014	30.1	78.4	0.38	3.40	3.13	1.09
	2015	29.9	78.2	0.38	3.40	3.14	1.08
	2016	20.2	78.9	0.26	2.85	3.14	0.91
	2017	20.5	78.5	0.26	2.99	3.09	0.97
Celtic Sea (IE)	2012	65.7	15.1	4.36	1.53	0.38	4.02
	2013	53.6	17.2	3.13	1.55	0.45	3.46
	2014	81.0	15.4	5.25	2.13	0.43	4.97
	2015	72.3	22.5	3.21	1.71	0.67	2.53
	2016	76.9	20.3	3.79	2.00	0.52	3.88
	2017	66.9	20.9	3.20	1.59	0.53	3.00
Celtic Sea (UK)	2012	51.4	128.9	0.40	1.69	7.01	0.24

RID area	Year	Total Nitrogen			Total Phosphorus		
		RID load	ICG-EMO load	Factor	RID load	ICG-EMO load	Factor
	2013	49.4	129.4	0.38	1.58	7.23	0.22
	2014	62.0	98.5	0.63	1.77	5.55	0.32
	2015	124.6	103.7	1.20	1.68	5.50	0.31
	2016	53.9	115.3	0.47	1.62	5.84	0.28
	2017	24.6	121.3	0.20	0.94	6.23	0.15
Channel and Irish Sea (FR)	2012	239.8	164.6	1.46	4.44	3.63	1.22
	2013	296.1	113.1	2.62	4.78	1.50	3.18
	2014	250.9	93.2	2.69	4.88	1.32	3.69
	2015	185.3	81.1	2.29	3.66	1.23	2.96
	2016	194.5	98.2	1.98	4.46	1.49	3.00
	2017	139.0	81.3	1.71	3.05	1.28	2.38
Channel (UK)	2012	41.5	69.6	0.60	1.53	3.23	0.47
	2013	38.2	66.9	0.57	1.33	3.07	0.43
	2014	47.0	28.1	1.67	1.51	1.22	1.24
	2015	32.8	33.3	0.98	1.22	1.51	0.81
	2016	34.3	47.3	0.73	0.88	2.21	0.40
	2017	20.7	47.8	0.43	0.47	2.25	0.21
Elbe	2012	87.7	92.5	0.95	4.36	4.98	0.87
	2013	165.6	117.8	1.41	6.11	4.00	1.53
	2014	65.4	95.3	0.69	3.56	5.44	0.65
	2015	66.2	92.3	0.72	4.35	6.26	0.69
	2016	72.6	100.8	0.72	3.90	5.60	0.69
	2017	85.0	105.7	0.80	4.75	5.75	0.83
Ems	2012	18.2	15.2	1.20	0.41	0.35	1.17
	2013	16.3	16.1	1.01	0.49	0.48	1.02
	2014	16.1	15.8	1.02	0.53	0.35	1.50
	2015	24.4	16.1	1.52	0.90	0.48	1.87
	2016	21.9	14.9	1.47	0.72	0.36	1.97
	2017	17.3	15.0	1.16	0.41	0.29	1.40
Humber	2012	76.5	92.9	0.82	3.43	4.72	0.73
	2013	71.7	92.2	0.78	2.60	4.43	0.59
	2014	76.4	55.2	1.38	2.67	1.41	1.89
	2015	51.2	50.1	1.02	2.38	1.73	1.38
	2016	65.0	58.5	1.11	1.95	1.60	1.22
	2017	51.3	71.8	0.71	2.04	2.18	0.94
Irish Sea (UK)	2012	30.8	5.1	5.99	1.89	0.11	16.59
	2013	26.7	5.3	5.06	1.76	0.12	14.89
	2014	37.0	4.2	8.78	2.04	0.11	18.55
	2015	28.3	5.1	5.58	1.16	0.14	8.01
	2016	22.6	5.1	4.47	0.93	0.15	6.22

RID area	Year	Total Nitrogen			Total Phosphorus		
		RID load	ICG-EMO load	Factor	RID load	ICG-EMO load	Factor
	2017	20.4	5.8	3.54	1.28	0.16	7.81
Irish Sea (UK)	2012	53.9	65.5	0.82	3.02	3.74	0.81
	2013	37.5	70.7	0.53	2.08	4.93	0.42
	2014	46.2	50.7	0.91	2.59	2.57	1.01
	2015	44.7	50.2	0.89	2.14	2.19	0.98
	2016	50.6	55.3	0.91	2.09	2.38	0.88
	2017	50.8	57.0	0.89	1.80	2.28	0.79
Kattegat (DK)	2012	20.6	8.8	2.33	0.74	0.36	2.06
	2013	18.2	10.7	1.70	0.60	0.38	1.58
	2014	22.0	9.5	2.32	0.73	0.33	2.18
	2015	25.2	7.1	3.53	0.86	0.27	3.22
	2016	20.6	6.9	2.96	0.70	0.27	2.60
	2017	21.4	7.3	2.92	0.75	0.30	2.54
North Sea (BE)	2012	32.1	30.9	1.04	2.80	2.97	0.94
	2013	34.5	28.3	1.22	2.24	2.40	0.93
	2014	25.8	26.0	0.99	2.11	2.39	0.88
	2015	26.5	26.3	1.01	1.96	2.29	0.86
	2016	30.7	30.6	1.00	2.40	2.19	1.10
	2017	17.8	23.4	0.76	1.37	2.30	0.60
North Sea (DE)	2012	3.7	10.1	0.37	0.22	0.55	0.40
	2013	3.6	10.2	0.36	0.23	0.56	0.41
	2014	3.6	10.0	0.36	0.20	0.55	0.37
	2015	4.5	10.4	0.43	0.26	0.57	0.46
	2016	3.6	9.7	0.37	0.20	0.54	0.37
	2017	4.7	9.7	0.48	0.34	0.54	0.62
North Sea (DK)	2012	18.8	13.5	1.39	0.60	0.57	1.07
	2013	15.8	14.2	1.11	0.50	0.56	0.90
	2014	17.1	13.2	1.29	0.54	0.51	1.07
	2015	19.3	11.7	1.64	0.57	0.41	1.37
	2016	15.7	12.9	1.22	0.46	0.47	0.97
	2017	17.1	13.0	1.32	0.49	0.45	1.07
North Sea (NL)	2012	233.5	249.2	0.94	7.50	10.41	0.72
	2013	273.8	266.7	1.03	9.45	12.16	0.78
	2014	214.7	241.9	0.89	8.76	11.22	0.78
	2015	163.4	243.3	0.67	6.23	11.72	0.53
	2016	255.7	247.5	1.03	7.45	10.05	0.74
	2017	191.1	237.3	0.81	4.62	9.24	0.50
North Sea (NO)	2012	47.2	2.4	19.96	4.18	0.04	112.31
	2013	43.1	2.4	18.18	4.04	0.04	108.74
	2014	45.6	2.4	19.35	4.12	0.04	109.67

RID area	Year	Total Nitrogen			Total Phosphorus		
		RID load	ICG-EMO load	Factor	RID load	ICG-EMO load	Factor
	2015	50.5	2.3	21.51	4.21	0.04	112.46
	2016	46.3	2.4	19.63	4.34	0.04	115.45
	2017	47.3	2.3	20.16	4.25	0.04	113.42
North Sea North (UK)	2012	66.7	64.6	1.03	5.39	3.03	1.78
	2013	49.0	67.0	0.73	3.61	3.72	0.97
	2014	58.6	54.2	1.08	4.18	3.07	1.36
	2015	55.7	55.6	1.00	3.95	3.12	1.27
	2016	37.6	60.4	0.62	2.38	3.35	0.71
	2017	30.4	58.6	0.52	1.85	3.07	0.60
Skagerrak (DK)	2012	1.2	1.7	0.73	0.07	0.13	0.52
	2013	1.1	2.2	0.52	0.05	0.12	0.43
	2014	1.4	1.6	0.91	0.07	0.10	0.70
	2015	1.5	1.1	1.32	0.07	0.07	0.92
	2016	1.4	1.5	0.90	0.06	0.08	0.76
	2017	1.6	1.7	0.96	0.07	0.09	0.79
Skagerrak (NO)	2012	41.3	25.4	1.63	1.41	0.81	1.74
	2013	39.2	25.2	1.56	1.06	0.66	1.61
	2014	44.1	25.1	1.76	1.24	0.67	1.84
	2015	42.9	25.3	1.69	1.16	0.68	1.71
	2016	35.8	25.4	1.41	0.92	0.68	1.36
	2017	38.3	25.4	1.51	0.98	0.68	1.45
Sweden total	2012	32.9	13.5	2.45	0.92	0.37	2.52
	2013	24.7	13.7	1.80	0.62	0.36	1.74
	2014	32.8	13.7	2.40	0.91	0.36	2.56
	2015	31.4	13.7	2.29	0.81	0.36	2.26
	2016	22.4	13.7	1.63	0.56	0.36	1.56
	2017	27.0	13.7	1.97	0.71	0.36	2.00
Thames	2012	39.2	61.5	0.64	3.07	5.25	0.59
	2013	38.3	52.4	0.73	2.93	3.62	0.81
	2014	48.8	30.7	1.59	3.75	1.91	1.96
	2015	27.8	31.3	0.89	3.24	2.28	1.42
	2016	12.7	36.7	0.35	0.60	2.60	0.23
	2017	17.1	45.3	0.38	0.34	3.55	0.10
Weser	2012	37.7	32.6	1.16	1.85	1.63	1.13
	2013	49.4	42.4	1.16	2.01	1.70	1.18
	2014	30.5	32.7	0.93	1.51	1.51	1.00
	2015	51.0	40.5	1.26	2.17	1.23	1.77
	2016	43.3	34.5	1.25	1.63	1.30	1.26

Deltares is an independent institute for applied research in the field of water and subsurface. Throughout the world, we work on smart solutions for people, environment and society.

Deltares

www.deltares.nl